Lehigh University
Lehigh Preserve

Fritz Laboratory Reports

Civil and Environmental Engineering

1972

Limit analysis solutions of earth pressure problems, May 1972 73-64

Jack L. Rosenfarb

F. Chen Wai

LIMIT ANALYSIS SOLUTIONS OF EARTH PRESSURE PROBLEMS

by

Jack L. Rosenfarb

Wai F. Chen

Fritz Engineering Laboratory
Department of Civil Engineering
Lehigh University
Bethlehem, Pennsylvania

May 1972

Fritz Engineering Laboratory Report No. 355.14

LIMIT ANALYSIS SOLUTIONS OF EARTH PRESSURE PROBLEMS

by

Jack L. Rosenfarb[1] and Wai F. Chen[2]

Key Words: earth pressures; cohesionless soil; limit-design method; plasticity; mechanism; design; soil mechanics

ABSTRACT:

The upper bound technique of limit analysis is used to obtain the active and passive limit earth pressures for a cohesionless soil retained by a rigid wall of varying roughness. The soil is treated as a perfectly plastic medium obeying the Mohr-Coulomb yield criterion and its associated flow rule. Various assumed failure mechanisms are evaluated. The resulting solutions are found to favorably agree with known solutions including those obtained by slip-line methods.

[1] Teaching Assistant, Department of Civil Engineering, Lehigh University, Bethlehem, Pa.

[2] Associate Professor of Civil Engineering, Fritz Laboratory, Lehigh University, Bethlehem, Pa.

TABLE OF CONTENTS

1. Introduction

The problem of the active and passive earth pressures acting on a rigid retaining wall has been studied ever since Coulomb formulated the limit equilibrium solutions in 1776 by assuming a simple straight failure line (Fig. 1(a)). It has long been recognized that such solutions greatly overestimate the passive pressure exerted on a relatively rough wall for high soil friction angles, e.g. φ = 30 to 40 degrees. Indeed for these situations the actual failure surface is far from straight but is curved. With the formulation of Kötter's curvilinear equilibrium equations came the complicated, numerically integrated, slipline solutions of Sokolovskii [21]. Although such solutions have been considered as "exact", it should be remembered that nowhere in the formulation has the soil deformation been considered, i.e. the soil stress-strain relationship.

With the development of the plastic limit theorems of perfect plasticity and their adaptation to the field of soil mechanics [10], many problems have been solved on a much more logical and simple basis through the concept of a flow rule or normality. This adaptation, called the limit analysis technique, has been successfully applied in obtaining solutions to the problems of slope stability [5,6,8] and bearing capacity [4].

The limit analysis technique has also been applied to obtain the active and passive earth pressures acting on a rigid retaining wall. Finn [11], and Chen and Scawthorn [7] have investigated the problem using the classical Coulomb straight line failure mechanism

(Fig. 1(a)) and simple discontinuous stress fields. A slightly more complicated mechanism consisting of two rigid sliding blocks (Fig. 1(b)) has briefly been discussed by Davis [9]. Some lower bound, straight line solutions, have been obtained by Lysmer [18] with the use of a computer technique somewhat related to the finite element method.

In the following work the upper bound technique of limit analysis is applied to obtain the upper bounds for the active and passive earth pressures acting on a rigid wall using various failure mechanisms (Fig. 1). A new circular shearing zone is also developed and is used in two new mechanisms as shown in Figures 1(d) and 1(f). Although the general formulation for a c - φ soil is presented, results are primarily discussed for a cohesionless soil with no surcharge on the backfill. The necessary additional equations for the inclusion of both cohesion and surcharge are however included in Appendix 1. As in Ref. [3] the soil is idealized as a perfectly plastic material which obeys the Coulomb yield condition and its associated flow rule.

2. Radial Shear Zone ($\varphi \neq 0$)

2.1 Velocity Field

A circular shearing zone for a soil with finite internal friction can be developed in a manner similar to that which was used in Ref. [3] for a log-spiral radial shearing zone. Consider a sector of a circle with central angle $\bar{\theta}$ to be composed of a series of n rigid triangles each of angle $\Delta\theta$, as shown in Fig. 2(a). The velocity vector of each triangle is directed at an angle φ to the discontinuous rigid boundary A-B-C-D-E as required by the associated flow rule idealization. Figure 2(b) shows the compatible velocity diagram for triangles AOB and BOC. It should be noted that the discontinuous velocity vector V_{o1} also makes an angle φ with the line OB. This vector is shown to be composed of components δu and δv parallel and perpendicular to the discontinuity OB. Thus δu can be considered as a simple slip velocity; while δv, a separation velocity. Assuming the central angle $\Delta\theta$ is sufficiently small we may write:

$$V_1 = V_o \frac{\cos(\frac{\Delta\theta}{2} - 2\varphi)}{\cos(\frac{\Delta\theta}{2} + 2\varphi)}$$

$$V_2 = V_1 \frac{\cos(\frac{\Delta\theta}{2} - 2\varphi)}{\cos(\frac{\Delta\theta}{2} + 2\varphi)}$$

$$\vdots \tag{1}$$

$$V_n = \frac{V_{n-1} \cos(\frac{\Delta\theta}{2} - 2\varphi)}{\cos(\frac{\Delta\theta}{2} + 2\varphi)}$$

The velocity in the nth triangle ODE can be expressed as

$$V_n = V_o \left[\frac{\cos(\frac{\Delta\theta}{2} - 2\varphi)}{\cos(\frac{\Delta\theta}{2} + 2\varphi)}\right]^n \tag{2}$$

where V_o is the initial zone velocity. The circular radial shearing zone will be obtained in the limit as the number of triangles grows to infinity. Equation 2 can be written as

$$V_o \left[\frac{\cos(\frac{\Delta\theta}{2} - 2\varphi)}{\cos(\frac{\Delta\theta}{2} + 2\varphi)}\right]^n = V_o \left[\frac{\cos(\frac{\bar{\theta}}{2n} - 2\varphi)}{\cos(\frac{\bar{\theta}}{2n} + 2\varphi)}\right]^n = V_o \left[\frac{1 + 2\tan\frac{\bar{\theta}}{2n}\tan 2\varphi}{1 - \tan\frac{\bar{\theta}}{2n}\tan 2\varphi}\right]^n$$

Now if $n \to \infty$ we obtain the limit

$$\lim_{n \to \infty} \left[1 + \frac{\bar{\theta}\tan 2\varphi}{n}\right]^n \quad \to \quad \exp(\bar{\theta}\tan 2\varphi)$$

or

$$V = V_o \exp(\theta \tan 2\varphi) \tag{3}$$

where V is the velocity at any location θ along the circular arc. Equation 3 is similar to the one derived for a log-spiral zone:

$$V = V_o \exp(\theta \tan\varphi) \tag{4}$$

2.2 Rate of Dissipation of Energy

The general formulation for the energy dissipation due to shearing for a Coulomb material has previously been developed [2,7]. In general, energy is dissipated along velocity discontinuities (narrow transition zones) and in the circular shearing zone. From Fig. 2(a) it is clear that this energy will be dissipated along radial and boundary surfaces. The rate of energy dissipation along a typical radial line, say OE, can be found by multiplying the cohesion C, discontinuity length r_o, and discontinuous tangential velocity $\delta u = V_{n,n+1}\cos\varphi$:

$$C\, r_o\, V_{n,n+1} \cos\varphi \tag{5}$$

Using Fig. 2(b) and assuming $\Delta\theta$ to be small, $\delta u = V_n\, \Delta\theta \cos\varphi/\cos 2\varphi$; and Eq. 5 can be written as:

$$\frac{C\, r_o\, V_n\, \Delta\theta \cos\varphi}{\cos 2\varphi} = \frac{C\, r_o\, V_o\, \Delta\theta \cos\varphi \exp(\theta \tan 2\varphi)}{\cos 2\varphi} \tag{6}$$

Integrating over the total circular radial shearing zone $\bar{\theta}$:

$$\frac{C\, r_o\, V_o \cos\varphi}{\sin 2\varphi}\left[\exp(\bar{\theta}\tan 2\varphi) - 1\right] \tag{7}$$

Likewise, the dissipation along a typical boundary surface, DE, is given by

$$C\left[2r_o \sin\frac{\Delta\theta}{2}\right] V_n \cos\varphi \tag{8}$$

which if $\Delta\theta$ is small becomes:

$$C\ r_o\ V_n\ \Delta\theta\ \cos\varphi = C\ r_o\ V_o\ \Delta\theta\ \cos\varphi\ \exp(\theta\ \tan 2\varphi) \tag{9}$$

Integrating over the total length A-B-C-D-E:

$$\frac{C\ r_o\ V_o\ \cos\varphi}{\tan 2\varphi}\left[\exp(\bar{\theta}\ \tan 2\varphi - 1)\right] \tag{10}$$

The corresponding total radial and boundary dissipation expressions for the log-spiral shearing zone are both equal to:

$$\frac{1}{2}\ C\ r_o\ V_o\ \cot\varphi\left[\exp(2\bar{\theta}\ \tan\varphi) - 1\right] \tag{11}$$

It is noted that for the circular zone this equality does not occur.

2.3 Rate of External Work

The external rate of work done by the soil weight in the circular zone can be computed by summing over the region $\bar{\theta}$ the products of each triangle's component of vertical velocity with its weight. Using Fig. 2(a) this can be expressed in integral form as:

$$\pm\frac{1}{2}\ \gamma\ V_o\ r_o^2 \int_o^{\bar{\theta}} \exp(\mp\ \theta\ \tan 2\varphi)\ \sin(\xi + \theta \mp \varphi - \frac{\pi}{2})\ d\theta \tag{12}$$

where the upper and lower signs signify the active and passive states respectively; and ξ denotes the angular inclination of the zone from the horizontal. The corresponding expression for the log-spiral zone is

$$\pm\frac{1}{2}\ \gamma\ V_o\ r_o^2 \int_o^{\bar{\theta}} \exp(\mp\ 3\theta\ \tan\varphi)\ \sin(\pi - \theta - \xi)\ d\theta \tag{13}$$

3. Log-Sandwich Mechanism

The upper bound theorem of limit analysis states that a soil mass will collapse if there is any compatible pattern of plastic deformation (velocity field or "mechanism") for which the rate of work of the external loads exceeds the rate of internal energy dissipation due to shearing of the soil. If a failure mechanism is described by n independent parameters, the active and passive pressures acting on a rigid wall can be expressed as:

$$P_a \;\alpha\; \text{Max}\left[K_{a\gamma}(\theta_1, \theta_2, \ldots \theta_n) + K_{aq}(\theta_1, \theta_2, \ldots \theta_n) + K_{ac}(\theta_1, \theta_2, \ldots \theta_n)\right]$$

$$P_p \;\alpha\; \text{Min}\left[K_{p\gamma}(\theta_1, \theta_2, \ldots \theta_n) + K_{pq}(\theta_1, \theta_2, \ldots \theta_n) + K_{pc}(\theta_1, \theta_2, \ldots \theta_n)\right] \tag{14}$$

where K_γ, K_q, and K_c are the coefficients representing the effects of weight, surcharge, and cohesion respectively; such that

$$P = \frac{1}{2}\gamma H^2 K_\gamma + qH K_q + cH K_c$$

A total of six different failure mechanisms, as shown in Fig. 1, are considered herein. Since the solution procedure for all cases is identical a detailed formulation will only be given for the log-sandwich mechanism and a cohesionless soil. The necessary equations for the inclusion of cohesion and surcharge loading are given in Appendix 1 while the two-triangle mechanism is discussed in Appendix 2.

Figure 3 shows a logarithmic spiral shearing zone, OBC, sandwiched between two rigid blocks, OAB and OCD. Since the velocities

V_1 and V_3 for the rigid triangles OAB and OCD are assumed perpendicular to the radial lines OB and OC, two angular parameters ρ and ψ describe the mechanism completely. It will be shown later that for certain limited boundary situations only one parameter need be considered. This simplification reduces the complexity of the solution process. The compatible velocity diagrams corresponding to the passive pressure case are given in Figs. 3(b) and 3(c) for the smooth ($\delta < \varphi$) and rough ($\delta = \varphi$) wall conditions respectively. Figure 4 shows the corresponding diagrams for the active case. The wall is assumed to translate horizontally with a velocity V_o. All other velocities in the mechanism can then be expressed in terms of V_o.

Rate of External Work

For a cohesionless soil with no surcharge loading, the rate of external work due to self-weight in any region is simply the vertical component of velocity in that region multiplied by the weight of the region: (Note: for passive case use lower signs)

Triangular region OAB:

$$\frac{\pm \frac{1}{2} \gamma H^2 V_1 \sin\rho \cos(\rho \pm \varphi) \cos(\alpha - \rho)}{\sin^2\alpha \cos\varphi} \tag{15}$$

Log-spiral region OBC: (see Eq. 13)

$$\frac{\frac{1}{2} \gamma H^2 V_1 \cos^2(\rho \pm \varphi)}{\sin^2\alpha \cos^2\varphi(1 + 9\tan^2\varphi)} \left\{\cos(\alpha - \rho)\left[\pm 3\tan\varphi + \left(\mp 3\tan\varphi \cos\psi + \sin\psi\right)\right.\right. \tag{16}$$

$$\left.\left.\exp(\mp 3\psi \tan\varphi)\right] + \sin(\alpha - \rho)\left[1 + \left(\mp 3\tan\varphi \sin\psi - \cos\psi\right) \exp(\mp 3\psi \tan\varphi)\right]\right\}$$

Triangular region OCD:

$$\frac{\pm \frac{1}{2} \gamma H^2 V_1 \cos^2(\rho \pm \varphi) \sin(\alpha - \rho - \Psi + \beta) \cos(\alpha - \rho - \Psi) \exp(\mp 3\Psi \tan\varphi)}{\sin^2\alpha \cos\varphi \cos(\alpha - \rho - \Psi + \beta \mp \varphi)} \quad (17)$$

External work is also done by the components of the resultant wall load P moving in the horizontal direction with velocity V_o:

$$\begin{Bmatrix} P_{aN} \\ P_{pN} \end{Bmatrix} V_o [\mp \sin\alpha + \tan\delta \cos\alpha] \quad (18)$$

where P_{aN} and P_{pN} are the normal to the wall components of the active and passive states respectively.

Rate of Internal Energy Dissipation

Since a cohesionless soil is being considered, the only dissipation occurs at the soil-wall interface. For a smooth wall ($\delta < \varphi$) the dissipation by sliding friction is given by

$$\begin{Bmatrix} P_{aN} \\ P_{pN} \end{Bmatrix} \tan\delta \, V_{01} \quad (19)$$

For a rough wall ($\delta = \varphi$) the internal dissipation of energy is 0 since $C = 0$ (see Eq. 5). Using the velocity diagrams, Figs. 3(b) and 3(c), or 4(b) and 4(c), the velocities V_1 and V_{01} can be expressed in terms of the translational wall velocity V_o for both smooth and rough cases in all the previous expressions. Equating the rate of external work to the rate of internal energy dissipation, a closed form expression for the resultant coefficients of active and passive pressures is obtained:

For a smooth wall:

$$\begin{Bmatrix} K_{a\gamma} \\ K_{p\gamma} \end{Bmatrix} = \frac{\mp \sec\delta}{\mp \sin\alpha + \tan\delta \cos\alpha - \dfrac{\tan\delta \cos(\alpha - \rho)}{\cos\rho}} \left\{ \frac{\tan\rho \cos(\rho \pm \varphi) \cos(\alpha - \rho)}{\sin\alpha \cos\varphi} \right.$$

$$+ \frac{\cos^2(\rho \pm \varphi)}{\cos\rho \sin\alpha \cos^2\varphi (1 + 9\tan^2\varphi)} \Big[\cos(\alpha - \rho) \; [\pm 3\tan\varphi + (\mp 3\tan\varphi \cos\psi + \sin\psi)$$

$$\exp(\mp 3\psi \tan\varphi)] + \sin(\alpha - \rho)[1 + (\mp 3\tan\varphi \sin\psi - \cos\psi) \exp(\mp 3\psi \tan\varphi)] \Big]$$

$$\left. + \frac{\cos^2(\rho \pm \varphi) \sin(\alpha - \rho - \psi + \beta) \cos(\alpha - \rho - \psi) \exp(\mp 3\psi \tan\varphi)}{\cos\varphi \sin\alpha \cos(\alpha - \rho - \psi \mp \varphi + \beta) \cos\rho} \right\} \qquad (20)$$

For a rough wall:

$$\begin{Bmatrix} K_{a\gamma} \\ K_{p\gamma} \end{Bmatrix} = \frac{\mp \sec\delta}{\mp \sin\alpha + \tan\delta \cos\alpha} \left\{ \frac{\sin^2\rho \cos(\rho \pm \varphi) \cos(\alpha - \rho) \sin(\alpha \mp \varphi)}{\sin^2\alpha \cos\varphi \cos(\rho \mp \varphi)} \right.$$

$$\mp \frac{\cos^2(\rho \pm \varphi) \sin(\alpha \mp \varphi)}{\sin^2\alpha \cos^2\varphi (1 + 9\tan^2\varphi) \cos(\rho \mp \varphi)} \Big[\cos(\alpha - \rho)[\pm 3\tan\varphi + (\mp 3\tan\varphi$$

$$\cos\psi + \sin\psi) \exp(\mp 3\psi \tan\varphi)] + \sin(\alpha - \rho)[1 + (\mp 3\tan\varphi \sin\psi - \cos\psi)$$

$$\exp(\mp 3\psi \tan\varphi)] \Big]$$

$$\left. + \frac{\cos^2(\rho \pm \varphi) \sin(\alpha - \rho - \psi + \beta) \cos(\alpha - \rho - \psi) \sin(\alpha \mp \varphi) \exp(\mp 3\psi \tan\varphi)}{\sin^2\alpha \cos\varphi \cos(\alpha - \rho - \psi + \beta \mp \varphi) \cos(\rho \mp \varphi)} \right\} \qquad (21)$$

In order to obtain the critical active and passive wall loads, expressions (20) and (21) must be either maximized or minimized respectively, with regard to the mechanism parameters ρ and ψ. This was accomplished with the aid of an iterative technique incorporating the method of steepest descent. Solutions were obtained on the CDC 6400 computer. A typical solution required at most 15 iterations or 0.1 seconds.

4. Discussion of Results

4.1 Passive Pressure

Table 1 shows the resultant passive pressure coefficients $K_{p\gamma}$ for three different wall inclinations α and a horizontal backfill ($\beta = 0$). These solutions were obtained by using the failure mechanisms given in Fig. 1. Mechanisms 3 and 4 failed to yield good solutions for the case of perfectly smooth walls ($\delta = 0$). It should be noted that these mechanisms cannot physically reduce down to the classical straight line failure mechanisms which effectively model smooth wall behavior. Figure 5(a) shows this reduction for the two-triangle mechanism (Mechanism 2) while Fig. 5(b) shows a similar reduction for the log-sandwich mechanism (Mechanism 5). In addition, for high soil friction angles ($\varphi = 40^{o}$) the arc-triangle mechanism (Mechanism 4) yielded poor results. This was expected due to the fact that the velocity in the circular radial shearing region approaches infinity as the region extent $\bar{\theta}$ approaches 45^{o}.

Solutions were found to be improved by the use of more elaborate mechanisms only for the case of rough walls retaining highly frictional backfills. For a soil with $\varphi = 40^{o}$ the solution obtained by using the log-sandwich mechanism was improved by 27% for the case of $\alpha = 110^{o}$, to as much as 78% for the vertical wall, $\alpha = 90^{o}$. The effect of wall roughness on the resulting passive pressure coefficients is shown in Fig. 6. For a horizontal backfill it is seen that roughness is particularly important for walls angled into a backfill of high soil friction angle. For a sloping backfill ($\beta = 20^o$) it is evident that roughness is important for all wall inclinations.

Mechanism 6 was identical to the log-sandwich mechanism except that the log-spiral region was replaced with the circular ($\varphi \neq 0$) shearing region discussed in Section 2. As before, results between the two compared favorably until high soil friction angles were encountered.

From these observations it is evident that Mechanisms 2 and 5 yielded the best solutions, with Mechanism 5 improving those solutions for rough walls. Although Mechanism 5 was physically more complicated, it was fully described by only two independent parameters as opposed to three for Mechanism 2. In an attempt to further reduce the number of parameters and hence simplify the minimization scheme, a study was made of the inclination of the straight line portion of the upper rigid body as it intersected the unloaded horizontal backfill surface (Fig. 1). Ideally for a Rankine failure state such lines should make angles of $\frac{\pi}{4} - \frac{\varphi}{2}$ with the horizontal. The results of this study are found in Table 2. Shown are the percent differences between the computed inclinations Ω and the theoretical Rankine inclinations; as well as the resulting differences in the coefficients $K_{p\gamma}$. It is interesting to note that for smooth walls inclined at $\alpha = 70^o$ considerable deviation occurred, but that such deviations resulted in no more than 7% difference in coefficient values. This fact illustrates the apparent insensitivity of the log-sandwich mechanism to changes in the angular extent of the rigid body adjoining the wall, since the log-spiral extent was virtually unaffected. It should be pointed out that the Rankine inclinations corresponded to coefficients which were greater than those obtained from the unconstrained log-sandwich mechanisms. If the mechanism is so constrained such that

$$\Omega = \frac{\pi}{2} - \alpha + \rho + \Psi - \varphi = \frac{\pi}{4} - \frac{\varphi}{2} \qquad (22)$$

we obtain one independent parameter:

$$\Psi = \alpha - \rho + \frac{\varphi}{2} - \frac{\pi}{4} \qquad (23)$$

where ρ is the angular extent of the rigid block adjoining the wall, and Ψ is angular extent of the log-spiral zone (Fig. 1(e)). Thus for horizontal backfills we can be assured that the resulting solutions will only slightly be in error.

For a backfill of varying inclination the Rankine state is defined by a line to the horizontal such that

$$\Omega = \frac{\pi}{4} - \frac{\varphi}{2} + \frac{\varepsilon}{2} - \frac{\beta}{2} \qquad (24)$$

where

$$\sin\varepsilon = \frac{\sin\beta}{\sin\varphi} \qquad (25)$$

and β is the backfill inclination from the horizontal. The usefullness of Eq. 24 was found to be limited only to the cases of soil friction angle φ less than 30° and backfill angle β less than 15°. For cases outside these limits the one-parameter solutions overestimated the corresponding two-parameter solutions by 5% to as much as 50%. The results given in Table 6 for sloping backfills therefore reflect the use of the two-parameter log-sandwich mechanism.

4.2 Active Pressure

Table 3 shows the resultant active pressure coefficients $K_{a\gamma}$ for three different wall inclinations and a horizontal backfill. These results correspond to the failure mechanisms given in Fig. 1. As in the case of passive pressure, Mechanisms 3 and 4 yielded poor solutions. Figures 7(a) and 7(b) show typical results for the two-triangle and log-sandwich mechanisms respectively. For the case of a vertical wall, $\alpha = 90^{\circ}$, both mechanisms yielded nearly identical results. For walls angled into the backfill ($\alpha = 110^{\circ}$), however, the log-sandwich mechanism underestimated the upper bound solution. Again the inclusion of a log-spiral zone in place of a circular shearing zone in the log-sandwich mechanism improves the solution. Table 2 shows that the Rankine condition at the unloaded surface was not as well obeyed as for the passive case. It should be noted, however, that the active mechanisms were much less sensitive in terms of final results, with a maximum deviation of not more than 5%. The number of independent parameters can also be reduced to one, such that

$$\Omega = \frac{\pi}{4} + \frac{\varphi}{2} - \frac{\varepsilon}{2} + \frac{\beta}{2} \tag{26}$$

where ε is defined by Eq. 25. As in the passive case the use of Eq. 26 results in poor values. For sloping backfills the two-parameter mechanism must again be used. The effect of wall roughness on the active pressure coefficients is shown in Fig. 8. Unlike the passive case for horizontal backfills, wall roughness has a much smaller effect and is important for walls angled out of the soil ($\alpha < 90^{\circ}$).

5. Comparison with Known Solutions

5.1 Passive Pressure

To date the best solutions have been generated by Sokolovskii [21] using the slip-line method or method of stress characteristics. For soils with weight, solutions are obtained by an approximate numerical integration of the characteristic stress equations of the plastic equilibrium field. The question of whether such a slip-line solution is either an upper or lower bound solution has already been discussed [4]. It is generally agreed, however, that such solutions give good estimates of the exact values. Table 4 shows a comparison of limit analysis solutions for horizontal backfills with those obtained by Sokolovskii. For the cases $\alpha = 70^{\circ}$ and $\alpha = 90^{\circ}$ (vertical wall) good agreement exists. It is also seen that the two-triangle and log-sandwich mechanisms control over the whole range of soil-wall conditions, especially for rough walls retaining soil of high friction angle ($\varphi = 30^{\circ}$ to 40°). For these cases the limit analysis method yields values which differ from the Sokolovskii solutions by no more than 15% ($\varphi = 40^{\circ}$, $\delta = 40^{\circ}$). For the case of the wall bearing into the backfill ($\alpha = 110^{\circ}$), considerably more disagreement occurred. The maximum difference obtained was 26.6% for the same case given above. It should be noted that the Sokolovskii solutions are very limited and easily available only for horizontal backfills. In a recent study by Lee and Herington [17] some slipline solutions for perfectly rough walls with sloping backfills have been formulated for both associated and non-associated flow rule materials.

Figure 9 shows a comparison of some typical limit analysis results for a vertical wall with several existing solutions. As previously mentioned the power of the method of limit analysis lies in the capability of bounding the true solution. Although lower bound solutions are much more difficult to obtain and involve the formulation of statically admissible stress fields, some limited solutions are available. As an example, for the particular case of a vertical wall with $\varphi = 40^{o}$, $\delta = 20^{o}$; a lower bound solution of 8.97 has been obtained by Lysmer [18]. The upper bound solution for this case is 10.10. The corresponding Sokolovskii solution of 9.69 is seen to lie between these two bounds. If an upper bound can be obtained that agrees with the corresponding lower bound solution, then of course, the exact solution will be found.

5.2 Active Pressure

A comparison of the active limit analysis solutions with those obtained by Sokolovskii is given in Table 5. In general the limit analysis results underestimate the slip-line solutions, with the greatest deviation being 6%. As in the case of passive pressures the log-sandwich and two-triangle mechanisms controlled in most cases. The exception to this, however, occurred for the case of the wall sloping into the earth backfill (i.e., $\alpha = 110^{o}$). The two-triangle mechanism yielded results which greatly exceeded the slip-line solutions. This was particularly true for the rough wall conditions i.e. $\delta = \varphi$. For these particular cases, however, the log-sandwich mechanism yielded much better agreement. The maximum deviation was reduced to 20%

($\varphi = 40^{\circ}$, $\delta = 40^{\circ}$). A comparison with some typical results is given in Fig. 10.

5.3 Cohesion and Surcharge

In order to illustrate the ease with which the effects of cohesion and surcharge are included in the analysis, two passive pressure example problems were solved using the expressions derived in Appendix 1.

The problem of a vertical wall retaining a c - φ soil was solved (Fig. 11(a)). A comparison with the trial wedge method shows excellent agreement. The problem of a wall retaining a cohesive, loaded soil is given in Fig. 11(b) which shows the resulting failure mechanisms for the effects of weight, cohesion, and surcharge. The final solution was obtained by superimposing these effects. As expected, the limit analysis method yielded lower solutions for highly frictional walls. For the particular problem solved ($\varphi = 20^{\circ}$, $\delta = 15^{\circ}$) the limit analysis solution was over 20% lower than the one obtained by using the graphical friction circle method.

6. Summary and Conclusions

It has been shown that the upper bound technique of limit analysis can yield rationally founded solutions that are in good agreement with the Sokolovskii slip-line results. In addition, these solutions are easily obtainable in a closed form. The formulation needed can be readily derived and has great physical appeal. A tabulation of passive pressure results for a cohensionless soil retained by a rigid wall of varying roughness δ and inclination α from the horizontal is given in Table 6. Table 7 shows the corresponding active pressure results.

The investigation of several assumed failure mechanisms has shown that significant solution improvement can especially be realized for the case of rough walls. These improvements have basically resulted from the use of new sandwich mechanism which incorporates a logarithmic spiral shearing zone. The use of this mechanism is particularly convenient and desirable due to the fact that only two independent parameters are needed in its description. An investigation was also made to study the effects of shifting the pole of the log-spiral region away from its position at the top of the wall. The resulting general sandwich mechanisms are shown in Fig. 12. From the results obtained it was concluded that very little solution improvement, if any, could be expected. Such improvement is outweighed by the complexity of the optimization procedure needed, since it must now contend with various functional discontinuities resulting from unknown velocity directions V_1 and V_3 as shown in Figs. 12(a) and 12(b) respectively. Improvement beyond the present stage may perhaps be realized only for other types of simple failure mechanisms.

It has also been shown that the simplicity of the upper bound technique makes it possible to easily include the effects of cohesion and surcharge. Such problems have previously been solved using the graphical forms of limit equilibrium. The problems of retaining walls with broken backs as well as backfills with irregular slopes can also be solved when appropriate kinematically admissible failure mechanisms are constructed. With the inclusion of non-homogeneous, layered soils for the limit analysis of slope stability problems [8], the extension to earth pressure situations is also possible.

7. Acknowledgments

The writers wish to acknowledge Misses Shirley Matlock and Phyllis Raudenbush for typing the manuscript; and Mrs. Sharon Balogh and Mr. John Gera for preparing the drawings.

8. References

1. Caquot, A., and Kerisel, J., Tables for the Calculation of Passive Pressure, Active Pressure, and Bearing Capacity of Foundations, Gauthier-Villars, Paris, 1948.

2. Chen, W. F., "On the Rate of Dissipation of Energy in Soils," Soils and Foundations, Vol. 8, No. 4, Dec. 1968, pp. 48-51.

3. Chen, W. F., "Soil Mechanics and Theorems of Limit Analysis," Journal of the Soil Mechanics and Foundations Division, ASCE, Vol. 95, No. SM2, Mar. 1969, pp. 493-518.

4. Chen, W. F., and Davidson, H. L., "Bearing Capacity Determination by Limit Analysis," Fritz Laboratory Report No. 355.15, Lehigh University, Bethlehem, Pennsylvania, Jan. 1972.

5. Chen, W. F., and Giger, M. W., "Limit Analysis of Stability of Slopes," Journal of the Soil Mechanics and Foundations Division, ASCE, Vol. 97, No. SM1, Jan. 1971.

6. Chen, W. F., Giger, M. W., and Fang, H. Y., "On the Limit Analysis of Stability of Slopes," Soils and Foundations, Vol. 9, No. 4, Dec. 1969.

7. Chen, W. F., and Scawthorn, C. R., "Limit Analysis and Limit Equilibrium Solutions in Soil Mechanics," Soils and Foundations, Vol. 10, No. 3, Sept. 1970, pp. 13-49.

8. Chen, W. F., Snitbhan, N., and Fang, H. Y., "Limit Analysis of Stability of Slopes in Anisotropic Non-Homogeneous Soils," Fritz Laboratory Report No. 355.13, Lehigh University, Bethlehem, Pennsylvania, Feb. 1972.

9. Davis, E. H., "Theories of Plasticity and the Failure of Soil Masses," Soil Mechanics--Selected Topics, I. K. Lee, ed., Chapter 6, American Elsevier, New York, 1968, pp. 341-380.

10. Drucker, D. C., and Prager, W., "Soil Mechanics and Plastic Analysis or Limit Design," Quarterly of Applied Mathematics, Vol. 10, No. 2, 1952, pp. 157-165.

11. Finn, W. D. Liam, "Applications of Limit Plasticity in Soil Mechanics," Journal of the Soil Mechanics and Foundations Division, ASCE, Vol. 93, No. SM5, Part 1, Sept. 1967, pp. 101-120.

12. Hansen, Brinch, Earth Pressure Calculation, Danish Technical Press, 1953.

13. Huntington, W. C., Earth Pressures and Retaining Walls, John Wiley and Sons, New York, 1961.

14. James, R. G., and Bransby, P. L., "Experimental and Theoretical Investigation of a Passive Earth Pressure Problem," Geotechnique, Vol. 20, No. 1, Mar. 1970, pp. 17-37.

15. James, R. G., and Bransby, P. L., "A Velocity Field for Some Passive Pressure Problems," Geotechnique, Vol. 21, No. 1, Mar. 1971, pp. 61-83.

16. Lee, I. K., and Herington, J. R., "The Effect of Wall Movement on Active and Passive Pressures," Uniciv Report No. R-71, University of New South Wales, Aug. 1971.

17. Lee, I. K., and Herington, J. R., "A Theoretical Study of the Pressures Acting on a Rigid Wall by a Sloping Earth or Rock Fill," Geotechnique, Vol. 22, No. 1, Mar. 1972, pp. 1-26.

18. Lysmer, J., "Limit Analysis of Plane Problems in Soil Mechanics," Journal of the Soil Mechanics and Foundations Division, ASCE, Vol. 96, No. SM4, July 1970, pp. 1311-1334.

19. Scott, R. F., "Plastic Equilibrium States in Soil," Principles of Soil Mechanics, Chapter 9, Addison-Wesley, Reading, 1963, pp. 398-427.

20. Shield, R. T., "Stress and Velocity Fields in Soil Mechanics," Journal of Mathematics and Physics, Vol. 33, No. 2, July 1954, pp. 144-156.

21. Sokolovskii, V. V., Statics of Granular Media, Pergamon Press, New York, 1965.

22. Terzaghi, K., Theoretical Soil Mechanics, John Wiley and Sons, New York, 1943.

23. Wu, T. H., "Plastic Equilibrium," Soil Mechanics, Chapter 8, Allyn and Bacon, Inc., Boston, 1964, pp. 252-264.

9. Notations

The following symbols are used in this report:

φ	internal friction angle of soil
γ	soil unit weight
C	soil cohesion
q	surcharge per unit width
H	vertical height of wall
α	angle of wall inclination
β	angle of backfill surface
δ	wall angle of friction
K_γ	coefficient of earth pressure due to weight
K_c	coefficient of earth pressure due to cohesion
K_q	coefficient of earth pressure due to surcharge
P_a, P_p	active and passive resultant earth pressures
P_{aN}, P_{pN}	normal active and passive earth pressures

ρ, Ψ, Ω	mechanism parameters
V_o	initial translational wall velocity
δu	discontinuous tangential velocity
r_o	initial radius of radial shear zone

Appendix 1

Log-Sandwich Mechanism

Cohesive Soil

For a cohesive soil, energy dissipation terms must be added for all surfaces of discontinuity as well as the shearing zone in the log-spiral region (Fig. 3). Since the line ABCD is continuous there will be no dissipation along either OB or OC due to a lack of relative movement at those surfaces. The following dissipation terms must, however, be included: (for passive case use lower signs)

Along the wall (OA) - see Eq. 19 for a smooth wall

For a rough wall ($\delta = \varphi$) the dissipation is given by

$$\frac{cH \cos\varphi \, V_{01}}{\sin\alpha} \tag{27}$$

Along AB

$$\frac{cH \sin\rho \, V_1}{\sin\alpha} \tag{28}$$

Along CD

$$\frac{cH \, V_1 \cos(\rho \pm \varphi) \sin(\alpha - \rho - \Psi + \beta) \exp(\mp \Psi \tan\varphi)}{\sin\alpha \cos(\alpha - \rho - \Psi \mp \varphi + \beta)} \tag{29}$$

From Eq. 11, the dissipation terms for shearing in the log-spiral zone and along the curved discontinuity BC are both equal to

$$\mp \frac{1}{2} \frac{cH V_1 \cos(\rho \pm \varphi)[\exp(\mp 2\psi \tan\varphi) - 1]}{\sin\varphi \sin\alpha} \tag{30}$$

Equating the rate of external work to the rate of internal energy dissipation:

For a smooth wall:

$$\begin{Bmatrix} K_{ac} \\ K_{pc} \end{Bmatrix} = \frac{\sec\delta}{\mp \sin\alpha + \tan\delta \cos\alpha - \dfrac{\tan\delta \cos(\alpha - \rho)}{\cos\rho}} \Bigg\{ \tan\rho$$

$$+ \frac{\cos(\rho \pm \varphi) \sin(\alpha - \rho - \psi + \beta) \exp(\mp \psi \tan\varphi)}{\cos\rho \cos(\alpha - \rho - \psi \mp \varphi + \beta)}$$

$$\mp \frac{\cos(\rho \pm \varphi)[\exp(\mp 2\psi \tan\varphi) - 1]}{\sin\varphi \cos\rho} \Bigg\} \tag{31}$$

For a rough wall:

$$\begin{Bmatrix} K_{ac} \\ K_{pc} \end{Bmatrix} = \frac{\sec\delta}{\mp \sin\alpha + \tan\delta \cos\alpha} \Bigg\{ \frac{\cos\varphi \cos(\alpha - \rho)}{\sin\alpha \cos(\rho \mp \varphi)} + \frac{\sin\rho \sin(\alpha \mp \varphi)}{\sin\alpha \cos(\rho \mp \varphi)}$$

$$+ \frac{\cos(\rho \pm \varphi) \sin(\alpha - \rho - \psi + \beta) \sin(\alpha \mp \varphi) \exp(\mp \psi \tan\varphi)}{\sin\alpha \cos(\alpha - \rho - \psi \mp \varphi + \beta) \cos(\rho \mp \varphi)}$$

$$\mp \frac{\cos(\rho \pm \varphi) \sin(\alpha \mp \varphi)[\exp(\mp 2\psi \tan\varphi) - 1]}{\sin\varphi \sin\alpha \cos(\rho \mp \varphi)} \Bigg\} \tag{32}$$

Surcharge

For a uniformly distributed surcharge loading q on the backfill as shown in Fig. 1, the following rate of external work term must be included:

$$\pm \frac{qH\, V_1 \cos(\rho \pm \varphi)\, \exp(\mp 2\psi \tan\varphi)}{\sin\alpha \cos(\alpha - \rho - \psi \mp \varphi + \beta)} \tag{33}$$

Equating the rate of external work to the rate of internal energy dissipation:

For a smooth wall:

$$\begin{Bmatrix} K_{aq} \\ K_{pq} \end{Bmatrix} = \frac{\mp \sec\delta}{\mp \sin\alpha + \tan\delta \cos\alpha - \frac{\tan\delta \cos(\alpha - \rho)}{\cos\rho}} \left\{ \frac{\cos(\rho \pm \varphi)\, \exp(\mp 2\psi \tan\varphi)}{\cos\rho \cos(\alpha - \rho - \psi \mp \varphi + \beta)} \right\} \tag{34}$$

For a rough wall:

$$\begin{Bmatrix} K_{aq} \\ K_{pq} \end{Bmatrix} = \frac{\mp \sec\delta}{\mp \sin\alpha + \tan\delta \cos\alpha} \left\{ \frac{\cos(\rho \pm \varphi)\, \sin(\alpha \mp \varphi)\, \exp(\mp 2\psi \tan\varphi)}{\sin\alpha \cos(\alpha - \rho - \psi \mp \varphi + \beta) \cos(\rho \mp \varphi)} \right\} \tag{35}$$

Appendix 2

Two-Triangle Mechanism

The two-triangle mechanism consists of two rigid sliding blocks and is completely described by three parameters (ρ, η, Ω). The velocity fields for both the passive and active states are shown in Figs. 13(a) and 13(b) respectively. The formulations for the coefficients of earth pressure due to weight, cohesion, and surcharge (K_γ, K_c, K_q) follow.

Rate of External Work

For a cohesionless soil with no surcharge loading, the rate of external work due to self-weight in any region is simply the vertical component of velocity in that region multiplied by the weight of the region: (Note: for passive case use lower signs)

Region OAB

$$\pm \frac{\frac{1}{2}\gamma H^2 V_1 \sin\rho \sin(\alpha + \eta) \sin(\eta \mp \varphi)}{\sin^2\alpha \sin(\alpha + \eta - \rho)} \qquad (36)$$

Region OBC

$$\pm \frac{\frac{1}{2}\gamma H^2 V_2 \sin^2(\alpha + \eta) \sin(\alpha - \rho + \beta) \sin(\alpha - \rho + \Omega) \sin(\Omega \mp \varphi)}{\sin^2\alpha \sin^2(\alpha + \eta - \rho) \sin(\Omega - \beta)}$$

Moving Wall Load - See Eq. 18

Rate of Energy Dissipation

For a smooth wall ($\delta < \varphi$) the dissipation by sliding friction is given by Eq. 19. For a rough wall ($\delta = \varphi$) the dissipation is given by Eq. 28.

With the use of the compatible velocity diagrams all velocities in the mechanism can be expressed in terms of the wall translational velocity V_o. For the case of smooth walls:

$$V_1 = \frac{V_o \sin\alpha}{\sin(\eta \mp \varphi + \alpha)} \qquad V_2 = \frac{V_o \sin\alpha \sin(\alpha - \rho + \eta \mp 2\varphi)}{\sin(\eta \mp \varphi + \alpha) \sin(\alpha - \rho + \Omega \mp 2\varphi)}$$

$$V_{o1} = \frac{V_o \sin(\eta \mp \varphi)}{\sin(\eta \mp \varphi + \alpha)} \qquad V_{12} = \frac{V_o \sin\alpha \sin(\Omega - \eta)}{\sin(\eta \mp \varphi + \alpha) \sin(\alpha - \rho + \Omega \mp 2\varphi)} \qquad (38)$$

For rough walls:

$$V_1 = \frac{V_o \sin(\alpha \mp \varphi)}{\sin(\eta + \alpha \mp 2\varphi)} \qquad V_2 = \frac{V_o \sin(\alpha \mp \varphi) \sin(\alpha + \eta - \rho \mp 2\varphi)}{\sin(\eta + \alpha \mp 2\varphi) \sin(\alpha - \rho + \Omega \mp 2\varphi)}$$

$$V_{o1} = \frac{V_o \sin(\eta \mp \varphi)}{\sin(\eta + \alpha \mp 2\varphi)} \qquad V_{12} = \frac{V_o \sin(\alpha \mp \varphi) \sin(\Omega - \eta)}{\sin(\eta + \alpha \mp 2\varphi) \sin(\alpha - \rho + \Omega \mp 2\varphi)} \qquad (39)$$

Equating the rate of external work to the rate of internal energy dissipation:

For a smooth wall:

$$\left\{\begin{matrix}K_{a\gamma}\\K_{p\gamma}\end{matrix}\right\} = \frac{\mp \sec\delta}{\mp \sin\alpha + \tan\delta \cos\alpha - \dfrac{\tan\delta \sin(\eta \mp \varphi)}{\sin(\eta \mp \varphi + \alpha)}}$$

$$\left\{\frac{\sin\rho \sin(\alpha + \eta) \sin(\eta \mp \varphi)}{\sin\alpha \sin(\alpha + \eta - \rho) \sin(\eta \mp \varphi + \alpha)}\right.$$

$$\left. + \frac{\sin^2(\alpha + \eta) \sin(\alpha - \rho + \beta) \sin(\alpha - \rho + \Omega) \sin(\Omega \mp \varphi) \sin(\alpha + \eta - \rho \mp 2\varphi)}{\sin\alpha \sin^2(\alpha + \eta - \rho) \sin(\Omega - \beta) \sin(\alpha + \eta \mp \varphi) \sin(\alpha - \rho + \Omega \mp 2\varphi)}\right\} \tag{40}$$

For a rough wall:

$$\left\{\begin{matrix}K_{a\gamma}\\K_{p\gamma}\end{matrix}\right\} = \frac{\mp \sec\delta}{\mp \sin\alpha + \tan\delta \cos\alpha} \left\{\frac{\sin\rho \sin(\alpha + \eta) \sin(\eta \mp \varphi) \sin(\alpha \mp \varphi)}{\sin^2\alpha \sin(\alpha + \eta - \rho) \sin(\eta + \alpha \mp 2\varphi)}\right.$$

$$\left. + \frac{\sin^2(\alpha+\eta) \sin(\alpha-\rho+\beta) \sin(\alpha-\rho+\Omega) \sin(\Omega\mp\varphi) \sin(\alpha\mp\varphi) \sin(\alpha+\eta-\rho\mp2\varphi)}{\sin^2\alpha \sin^2(\alpha+\eta-\rho) \sin(\Omega-\beta) \sin(\eta+\alpha\mp2\varphi) \sin(\alpha-\rho+\Omega\mp2\varphi)}\right\} \tag{41}$$

Cohesive Soil

The following dissipation expressions are necessary:

Along the wall (OA) - see expressions (19) and (27)

Along AB

$$\frac{cH V_1 \cos\varphi \sin\rho}{\sin\alpha \sin(\alpha+\eta-\rho)} \tag{42}$$

Along OB

$$\frac{cH V_{12} \cos\varphi \sin(\alpha+\eta)}{\sin\alpha \sin(\alpha+\eta-\rho)} \tag{43}$$

Along BC

$$\frac{cH V_2 \cos\varphi \sin(\alpha+\eta) \sin(\alpha-\rho+\beta)}{\sin\alpha \sin(\alpha+\eta-\rho) \sin(\Omega-\beta)} \tag{44}$$

For a smooth wall:

$$\begin{Bmatrix} K_{ac} \\ K_{pc} \end{Bmatrix} = \frac{\sec\delta}{\mp \sin\alpha + \tan\delta \cos\alpha - \dfrac{\tan\delta \sin(\eta\mp\varphi)}{\sin(\eta\mp\varphi+\alpha)}}$$

$$\left\{ \frac{\cos\varphi \sin\rho}{\sin(\eta\mp\varphi+\alpha)\ \sin(\alpha+\eta-\rho)} + \frac{\cos\varphi \sin(\alpha+\eta) \sin(\Omega-\eta)}{\sin(\alpha+\eta-\rho)\ \sin(\eta\mp\varphi+\alpha)\ \sin(\alpha-\rho+\Omega\mp 2\varphi)} \right. \qquad (45)$$

$$\left. + \frac{\cos\varphi \sin(\alpha+\eta) \sin(\alpha-\rho+\beta) \sin(\alpha+\eta-\rho\mp 2\varphi)}{\sin(\alpha+\eta-\rho)\ \sin(\Omega-\beta)\ \sin(\eta\mp\varphi+\alpha)\ \sin(\alpha-\rho+\Omega\mp 2\varphi)} \right\}$$

For a rough wall:

$$\begin{Bmatrix} K_{ac} \\ K_{pc} \end{Bmatrix} = \frac{\cos\delta}{\mp \sin\alpha + \tan\delta \cos\alpha} \left\{ \frac{\cos\varphi \sin(\eta\mp\varphi)}{\sin\alpha\ \sin(\eta+\alpha\mp 2\varphi)} + \frac{\cos\varphi \sin\rho \sin(\alpha\mp\varphi)}{\sin\alpha\ \sin(\alpha+\eta-\rho)\ \sin(\eta+\alpha\mp 2\varphi)} \right.$$

$$+ \frac{\cos\varphi \sin(\alpha+\eta) \sin(\alpha\mp\varphi) \sin(\Omega-\eta)}{\sin\alpha\ \sin(\alpha+\eta-\rho)\ \sin(\eta+\alpha\mp 2\varphi)\ \sin(\alpha-\rho+\Omega\mp 2\varphi} \qquad (46)$$

$$\left. + \frac{\cos\varphi \sin(\alpha+\eta) \sin(\alpha-\rho+\beta) \sin(\alpha\mp\varphi) \sin(\alpha+\eta-\rho\mp 2\varphi)}{\sin\alpha\ \sin(\alpha+\eta-\rho)\ \sin(\Omega-\beta)\ \sin(\eta+\alpha\mp 2\varphi)\ \sin(\alpha-\rho+\Omega\mp 2\varphi)} \right\}$$

Surcharge Loading

The following rate of external work term is necessary for a backfill uniformly loaded with a surcharge q:

$$\frac{\pm qH\ V_2 \sin(\alpha+\eta) \sin(\alpha-\rho+\Omega) \sin(\Omega\mp\varphi)}{\sin\alpha\ \sin(\alpha+\eta-\rho)\ \sin(\Omega-\beta)} \qquad (47)$$

For a smooth wall:

$$\begin{Bmatrix} K_{aq} \\ K_{pq} \end{Bmatrix} = \frac{\mp \sec\delta}{\mp \sin\alpha + \tan\delta \cos\alpha - \dfrac{\tan\delta \sin(\eta\mp\varphi)}{\sin(\eta\mp\varphi+\alpha)}} \qquad (48)$$

$$\left\{ \frac{\sin(\alpha+\eta) \sin(\alpha-\rho+\Omega) \sin(\Omega\mp\varphi) \sin(\alpha+\eta-\rho\mp 2\varphi)}{\sin(\alpha+\eta-\rho)\ \sin(\Omega-\beta)\ \sin(\eta\mp\varphi+\alpha)\ \sin(\alpha-\rho+\Omega\mp 2\varphi)} \right\}$$

<u>For a rough wall</u>:

$$\left\{ \begin{matrix} K_{aq} \\ K_{pq} \end{matrix} \right\} = \frac{\mp \sec\delta}{\mp \sin\alpha + \tan\delta \cos\alpha} \tag{49}$$

$$\left\{ \frac{\sin(\alpha+\eta)\ \sin(\alpha\mp\varphi)\ \sin(\alpha-\rho+\Omega)\ \sin(\Omega\mp\varphi)\ \sin(\alpha+\eta-\rho\mp 2\varphi)}{\sin\alpha\ \sin(\alpha+\eta-\rho)\ \sin(\Omega-\beta)\ \sin(\eta+\alpha\mp 2\varphi)\ \sin(\alpha-\rho+\Omega\mp 2\varphi)} \right\}$$

Table 1 Passive Pressure Coefficients $K_{p\gamma}$ (β = 0)

	φ	δ	Mechanism (1)	(2)	(3)	(4)	(5)	(6)
α = 70	10	0	1.36	1.36	1.52	1.47	1.36	1.36
		5	1.45	1.46	1.53	1.50	1.45	1.45
		10	1.55	1.54	1.54	1.54	1.54	1.54
	20	0	1.75	1.75	2.31	2.01	1.75	1.75
		10	2.08	2.08	2.36	2.18	2.08	2.08
		20	2.49	2.44	2.46	2.47	2.44	2.47
	30	0	2.27	2.28	3.86	2.75	2.28	2.30
		15	3.16	3.16	4.06	3.36	3.16	3.18
		30	4.76	4.43	4.50	4.76	4.41	4.76
	40	0	3.02	3.02	7.76	3.52	3.02	3.27
		20	5.34	5.32	8.33	5.39	5.31	5.89
		40	12.80	10.00	10.10	15.50	9.88	--
α = 90	10	0	1.42	1.42	1.68	1.60	1.42	1.42
		5	1.57	1.56	1.69	1.63	1.56	1.56
		10	1.73	1.68	1.71	1.68	1.68	1.67
	20	0	2.04	2.04	3.07	2.60	2.04	2.04
		10	2.64	2.58	3.12	2.82	2.58	2.61
		20	3.53	3.18	3.27	3.19	3.17	3.19
	30	0	3.00	3.00	6.38	4.80	3.00	3.01
		15	4.98	4.71	6.61	5.88	4.71	4.97
		30	10.10	7.24	7.37	8.31	7.10	8.31
	40	0	4.60	4.61	16.10	15.40	4.60	4.67
		20	11.80	10.10	17.70	23.60	10.10	12.50
		40	92.60	22.70	21.70	67.90	20.90	--
α = 110	10	0	1.76	1.74	3.10	2.06	1.74	1.74
		5	1.90	1.83	3.12	1.97	1.96	1.96
		10	2.04	1.91	2.77	1.90	2.16	2.14
	20	0	2.98	2.91	6.41	4.03	2.91	2.93
		10	3.78	3.38	6.50	3.85	3.91	3.94
		20	4.81	3.92	5.22	3.79	5.04	4.95
	30	0	5.34	5.09	15.60	10.20	5.08	5.33
		15	9.22	6.99	16.10	10.10	8.93	10.20
		30	72.70	10.10	11.70	11.50	14.40	17.60
	40	0	10.70	9.73	50.30	127.00	9.71	11.40
		20	89.70	17.60	53.50	141.00	25.50	69.40
		40	77.40	--	34.90	298.00	56.60	--

Table 2 Effects of Rankine Constraint (β = 0)

	φ	δ	Passive Log-Sandwich Ω % Diff.	Passive Log-Sandwich $K_{p\gamma}$ % Diff.	Active Log-Sandwich Ω % Diff.	Active Log-Sandwich $K_{a\gamma}$ % Diff.
α = 70	10	0	26.30	1.47	20.00	--
		5	--	--	9.20	--
		10	1.00	--	40.00	--
	20	0	27.40	2.24	18.40	1.85
		10	--	--	6.00	--
		20	2.28	--	3.82	--
	30	0	36.00	3.94	16.80	3.02
		15	1.66	--	9.00	--
		30	2.00	--	3.50	--
	40	0	35.60	6.64	6.85	4.80
		20	1.60	--	21.60	--
		40	2.40	--	6.15	--
α = 90	10	0	2.00	--	1.40	--
		5	2.00	--	--	--
		10	1.00	--	--	--
	20	0	--	--	1.27	--
		10	--	--	--	--
		20	2.57	--	--	--
	30	0	--	--	1.17	--
		15	1.33	--	2.16	--
		30	2.00	--	--	--
	40	0	2.40	--	1.07	--
		20	4.40	--	--	--
		40	7.00	--	--	--
α = 110	10	0	1.75	--	--	--
		5	--	--	8.60	--
		10	2.25	--	4.20	--
	20	0	1.15	--	1.82	--
		10	4.56	--	1.09	--
		20	6.30	--	7.82	--
	30	0	1.33	--	17.50	--
		15	5.66	--	.50	--
		30	--	--	10.00	--
	40	0	--	--	4.31	--
		20	--	--	14.50	--
		40	--	--	.46	--

Table 3 Active Pressure Coefficients $K_{a\gamma}$ ($\beta = 0$)

α	φ	δ	Mechanism (1)	(2)	(3)	(4)	(5)	(6)
α = 70	10	0	.833	.821	.774	.738	.832	.832
		5	.801	.800	.775	.778	.801	.801
		10	.786	.787	.786	.826	.787	.786
	20	0	.648	.616	.576	.447	.647	.647
		10	.615	.610	.582	.485	.615	.614
		20	.613	.614	.613	.549	.613	.613
	30	0	.498	.490	.434	.173	.497	.497
		15	.476	.473	.446	.187	.475	.475
		30	.501	.501	.501	.230	.501	.501
	40	0	.375	.320	.328	--	.375	.373
		20	.370	.303	.346	--	.368	.365
		40	.428	.417	.428	--	.428	.418
α = 90	10	0	.704	.704	.622	.572	.704	.704
		5	.662	.664	.624	.566	.664	.663
		10	.635	.642	.631	.564	.642	.637
	20	0	.490	.490	.394	.236	.490	.490
		10	.447	.448	.400	.226	.448	.447
		20	.427	.434	.420	.222	.434	.427
	30	0	.333	.333	.250	--	.333	.333
		15	.301	.302	.259	--	.302	.301
		30	.297	.303	.289	--	.302	.297
	40	0	.217	.215	.155	--	.217	.217
		20	.199	.200	.165	--	.200	.197
		40	.210	.214	.202	--	.214	.210
α = 110	10	0	.644	.649	1.09	.441	.649	.647
		5	.625	.639	1.09	.436	.601	.595
		10	.616	.649	1.26	.435	.569	.561
	20	0	.380	.387	.679	.015	.385	.382
		10	.371	.386	.689	--	.341	.353
		20	.378	.417	.943	--	.319	.307
	30	0	.212	.218	.434	--	.216	.212
		15	.215	.226	.449	--	.188	.181
		30	.237	.275	.767	--	.178	.168
	40	0	.106	.111	.280	--	.109	.106
		20	.115	.123	.298	--	.095	.090
		40	.146	.180	.687	--	.095	.088

Table 4 Comparison with Passive Slip-line Solutions (β = 0)

	φ	δ	$K_{p\gamma}$ Sokolovskii(21)	$K_{p\gamma}$ Limit Analysis	Mechanism	% Diff.
α = 70	10	0	1.34	1.36	1,2,5,6	+ 1.49
		5	1.46	1.45	1,2,5,6	- .68
		10	1.53	1.54	1,2,3,4,5,6	+ .65
	20	0	1.71	1.75	1,2,5,6	+ 2.34
		10	2.08	2.08	1,2,5,6	--
		20	2.42	2.44	2,5	+ .83
	30	0	2.16	2.28	1,2,5	+ 7.86
		15	3.16	3.16	1,2,5	--
		30	4.30	4.41	5	+ 2.56
	40	0	2.84	3.02	1,2,5	+ 6.34
		20	5.32	5.31	2,5	- 2.07
		40	9.32	9.88	5	+ 6.00
α = 90	10	0	1.42	1.42	1,2,5,6	--
		5	1.56	1.56	1,2,5,6	--
		10	1.66	1.68	2,4,5,6	+ 1.20
	20	0	2.04	2.04	1,2,5,6	--
		10	2.55	2.58	2,5	+ 1.18
		20	3.04	3.17	2,5	+ 4.27
	30	0	3.00	3.00	1,2,5,6	--
		15	4.62	4.71	2,5	+ 1.95
		30	6.55	7.10	5	+ 8.40
	40	0	4.60	4.60	1,2,5	--
		20	9.69	10.10	2,5	+ 4.23
		40	18.20	20.90	5	+14.85
α = 110	10	0	1.75	1.74	2,5,6	- .57
		5	1.95	1.83	2	- 6.15
		10	2.10	1.90	2,4	- 9.50
	20	0	2.90	2.91	2,5	+ .34
		10	3.80	3.38	2	-11.00
		20	4.62	3.79	4	-18.00
	30	0	5.06	5.08	2,5	+ .40
		15	8.45	8.93	5	+ 5.65
		30	12.30	14.40	5	+17.10
	40	0	9.56	9.71	5	+ 1.57
		20	22.40	25.50	5	+13.80
		40	44.70	56.60	5	+26.60

Table 5 Comparison with Active Slip-line Solutions ($\beta = 0$)

	φ	δ	$K_{a\gamma}$ Sokolovskii(21)	$K_{a\gamma}$ Limit Analysis	Mechanism	% Diff.
$\alpha = 70$	10	0	.826	.833	1,5,6	+ .85
		5	.794	.801	1,2,5,6	+ .88
		10	.794	.787	1,2,3,5,6	- .88
	20	0	.656	.648	1,5,6	- 1.21
		10	.612	.615	1,5,6	+ .49
		20	.612	.614	1,2,5,6	+ .33
	30	0	.521	.498	1,5,6	- 4.41
		15	.487	.476	1,5,6	- 2.26
		30	.510	.501	1,2,3,5,6	- 1.76
	40	0	.396	.375	1,5	- 5.30
		20	.385	.370	1	- 3.90
		40	.430	.428	1,3,5	- .47
$\alpha = 90$	10	0	.700	.704	1,2,5,6	+ .57
		5	.670	.664	2,5	- .89
		10	.650	.642	2,5	- 1.23
	20	0	.490	.490	1,2,5,6	--
		10	.450	.448	2,5	- .44
		20	.440	.434	2,5	- 1.36
	30	0	.330	.333	1,2,5,6	+ .91
		15	.300	.302	2,5	+ .67
		30	.310	.303	2	- 2.26
	40	0	.220	.217	1,5,6	- 1.36
		20	.200	.200	2,5	--
		40	.220	.214	2,5	- 2.73
$\alpha = 110$	10	0	.665	.649	2,5	- 2.40
		5	.620	.639	2	- 3.06
		10	.596	.649	2	+ 8.90
	20	0	.482	.387	2	- 1.98
		10	.356	.386	2	+ .84
		20	.344	.417	2	+21.20
	30	0	.229	.218	2	- 4.81
		15	.206	.226	2	+ 9.71
		30	.195	.275	2	+41.00
	40	0	.126	.111	2	-11.90
		20	.106	.123	2	+16.00
		40	.119	.180	2	+51.30

Table 6 Passive Earth Pressure Coefficients $K_{P\gamma}$

Angle of internal friction φ(deg)	Wall friction angle δ(deg)	Backfill angle β(deg)	Wall Angle α (deg.) 50	60	70	80	90	100	110	120	130
10	0	0	1.58	1.44	1.38	1.37	1.42	1.54	1.74	2.06	2.60
		10	1.87	1.69	1.62	1.61	1.68	1.81	2.05	2.45	3.11
	5	0	1.61	1.50	1.45	1.48	1.56	1.71	1.96	2.36	3.03
		10	2.05	1.87	1.80	1.81	1.90	2.08	2.39	2.89	3.74
	10	0	1.66	1.56	1.54	1.58	1.68	1.87	2.16	2.64	3.45
		10	2.19	2.01	1.95	1.98	2.10	2.32	2.70	3.31	4.35
15	0	0	1.75	1.62	1.57	1.59	1.70	1.91	2.24	2.78	3.70
		10	2.08	1.92	1.88	1.93	2.07	2.32	2.74	3.43	4.61
	5	0	1.78	1.68	1.67	1.74	1.89	2.15	2.57	3.24	4.40
		10	2.27	2.13	2.10	2.18	2.36	2.69	3.22	4.10	5.62
	10	0	1.84	1.77	1.79	1.89	2.08	2.40	2.90	3.72	5.13
		10	2.46	2.32	2.32	2.43	2.66	3.07	3.72	4.81	6.69
	15	0	1.91	1.87	1.91	2.04	2.27	2.64	3.23	4.20	5.87
		10	2.63	2.50	2.52	2.66	2.95	3.44	4.22	5.52	7.79
20	0	0	1.92	1.81	1.79	1.86	2.04	2.37	2.91	3.78	5.32
		10	2.29	2.17	2.18	2.30	2.56	2.98	3.68	4.85	6.91
		20	2.78	2.62	2.62	2.77	3.09	3.63	4.50	5.98	8.63
	5	0	1.98	1.90	1.92	2.04	2.30	2.72	3.39	4.49	6.45
		10	2.52	2.41	2.45	2.63	2.96	3.51	4.40	5.90	8.57
		20	3.14	2.99	3.02	3.24	3.65	4.35	5.49	7.42	10.9
	10	0	2.05	2.01	2.08	2.26	2.58	3.09	3.91	5.27	7.69
		10	2.75	2.67	2.75	2.98	3.39	4.08	5.19	7.05	10.4
		20	3.52	3.37	3.45	3.73	4.26	5.13	6.57	9.01	13.4
	15	0	2.14	2.14	2.26	2.49	2.88	3.49	4.47	6.11	9.04
		10	2.99	2.93	3.05	3.34	3.85	4.68	6.02	8.29	12.4
		20	3.90	3.77	3.89	4.25	4.90	5.97	7.73	10.7	16.4
	20	0	2.26	2.29	2.44	2.71	3.17	3.89	5.04	6.95	10.4
		10	3.22	3.19	3.34	3.70	4.30	5.29	6.95	9.65	14.0
		20	4.26	4.15	4.32	4.77	5.55	6.83	8.94	12.5	18.9
25	0	0	2.14	2.05	2.06	2.18	2.46	2.98	3.81	5.23	7.80
		10	2.54	2.46	2.53	2.76	3.18	3.88	5.02	6.99	10.6
		20	3.15	3.04	3.14	3.44	4.00	4.91	6.43	9.06	13.9
	5	0	2.21	2.15	2.22	2.42	2.82	3.47	4.53	6.33	9.64
		10	2.81	2.75	2.88	3.19	3.74	4.63	6.11	8.66	13.4
		20	3.58	3.50	3.66	4.07	4.80	5.99	7.98	11.4	17.8
	10	0	2.30	2.29	2.42	2.72	3.22	4.02	5.34	7.60	11.8
		10	3.08	3.07	3.27	3.76	4.36	5.49	7.35	10.6	16.6
		20	4.04	4.00	4.24	4.78	5.70	7.23	9.75	14.1	22.4

Table 6 Passive Earth Pressure Coefficients $K_{p\gamma}$

φ	δ	β	α 50	60	70	80	90	100	110	120	130
25	15	0	2.41	2.46	2.67	3.05	3.66	4.64	6.25	9.02	14.2
		10	3.39	3.43	3.69	4.20	5.05	6.44	8.74	12.7	20.2
		20	4.54	4.55	4.87	5.55	6.70	8.59	11.7	17.2	27.4
	20	0	2.56	2.67	2.94	3.40	4.13	5.31	7.23	10.6	16.8
		10	3.72	3.80	4.13	4.76	5.80	7.47	10.4	15.3	24.5
		20	5.07	5.12	5.55	6.38	7.79	10.1	14.5	21.4	34.5
	25	0	2.74	2.89	3.21	3.76	4.62	6.00	8.26	12.2	19.5
		10	4.05	4.18	4.59	5.34	6.57	8.54	12.0	17.8	29.7
		20	5.60	5.71	6.23	7.24	8.90	11.6	16.8	25.0	40.4
30	0	0	2.37	2.31	2.37	2.57	3.00	3.78	5.08	7.37	11.7
		10	2.82	2.79	2.95	3.34	4.01	5.12	7.00	10.3	16.8
		20	3.57	3.54	3.79	4.32	5.25	6.79	9.43	14.2	23.3
		30	4.41	4.42	4.76	5.68	6.74	8.82	12.4	18.8	31.3
	5	0	2.46	2.44	2.57	2.88	3.49	4.49	6.16	9.13	14.8
		10	3.13	3.15	3.40	3.92	4.79	6.24	8.70	13.1	21.6
		20	4.07	4.12	4.48	5.19	6.42	8.46	11.9	18.2	30.4
		30	5.19	5.26	5.76	6.79	8.39	11.2	16.0	24.5	41.3
	10	0	2.57	2.61	2.82	3.29	4.06	5.32	7.44	11.2	18.5
		10	3.47	3.55	3.91	4.58	5.70	7.56	10.7	16.4	27.4
		20	4.66	4.78	5.27	6.21	7.79	10.4	14.9	23.0	38.9
		30	6.07	6.23	6.90	8.02	10.3	14.0	20.1	31.3	53.2
	15	0	2.72	2.83	3.16	3.75	4.71	6.27	8.92	13.7	22.9
		10	3.85	4.02	4.50	5.34	6.75	9.08	13.0	20.2	34.1
		20	5.31	5.52	6.17	7.37	9.37	12.7	18.4	28.7	48.7
		30	7.05	7.32	8.21	10.3	12.6	17.2	25.0	39.2	66.0
	20	0	2.91	3.11	3.55	4.27	5.44	7.36	10.6	16.4	27.8
		10	4.29	4.54	5.15	6.20	7.94	10.8	16.1	25.2	42.9
		20	6.03	6.35	7.18	8.68	11.2	15.3	23.0	37.0	63.0
		30	8.14	8.54	9.68	12.3	15.1	20.8	30.5	49.0	82.0
	25	0	3.15	3.44	3.97	4.85	6.25	8.55	12.5	19.5	33.2
		10	4.77	5.11	5.86	7.14	9.24	12.7	19.1	30.1	51.4
		20	6.81	7.25	8.29	10.1	13.1	18.1	27.5	44.0	78.5
		30	9.32	9.87	11.3	14.4	17.9	25.0	37.6	60.0	100.
	30	0	3.42	3.77	4.41	5.45	7.10	9.80	14.4	22.7	38.8
		10	5.26	5.70	6.60	8.13	10.6	15.1	22.2	35.1	60.3
		20	7.62	8.18	9.44	11.6	15.2	21.4	32.8	54.0	94.0
		30	10.5	11.2	13.0	16.7	20.8	29.0	44.0	72.4	122.
35	0	0	2.67	2.64	2.76	3.07	3.69	4.87	6.92	10.7	18.3
		10	3.14	3.19	3.47	4.07	5.20	6.90	10.0	15.9	27.7
		20	4.06	4.14	4.60	5.56	7.03	9.66	14.3	23.0	40.9

Table 6 Passive Earth Pressure Coefficients $K_{p\gamma}$

φ	δ	β	α 50	60	70	80	90	100	110	120	130
35	0	30	5.17	5.37	6.10	7.40	9.50	13.3	20.0	32.7	56.0
	5	0	2.78	2.81	3.01	3.47	4.37	5.91	8.60	13.6	23.7
		10	3.50	3.63	4.05	4.86	6.25	8.61	12.8	20.6	36.5
		20	4.66	4.88	5.53	6.60	8.79	12.3	18.6	30.4	54.5
		30	6.14	6.49	7.50	9.20	12.2	17.2	26.4	43.6	78.4
	10	0	2.92	3.02	3.34	4.01	5.19	7.17	10.7	17.2	30.4
		10	3.92	4.14	4.74	5.81	7.61	10.7	16.1	26.4	47.4
		20	5.39	5.75	6.64	8.20	10.9	15.6	23.8	39.4	71.3
		30	7.29	7.82	9.00	11.2	14.7	21.2	34.1	56.9	110.
	15	0	3.10	3.29	3.77	4.67	6.16	8.68	13.1	21.5	38.6
		10	4.40	4.76	5.55	6.93	9.24	13.2	20.2	33.5	60.6
		20	6.25	6.77	7.94	10.0	13.5	19.5	30.1	50.3	91.6
		30	8.63	9.41	11.0	13.8	18.5	27.0	43.5	73.0	138.
	20	0	3.33	3.64	4.32	5.44	7.31	10.5	16.1	26.6	48.2
		10	4.97	5.48	6.49	8.24	11.2	16.1	26.0	43.5	79.2
		20	7.23	7.96	9.48	12.0	16.5	24.1	38.7	66.0	118.
		30	10.2	11.2	13.4	17.0	23.2	34.5	55.0	96.0	175.
	25	0	3.63	4.10	4.94	6.33	8.63	12.5	19.4	32.5	59.2
		10	5.63	6.30	7.58	9.75	13.4	19.5	31.7	53.4	97.7
		20	8.35	9.32	11.2	14.2	20.0	29.4	46.8	81.0	148.
		30	11.9	13.3	16.2	20.8	29.0	43.0	70.0	122.	225.
	30	0	4.01	4.61	5.64	7.33	10.1	14.8	23.2	39.0	71.4
		10	6.36	7.21	8.79	11.4	15.8	24.2	38.0	64.3	118.
		20	9.59	10.8	13.2	16.8	23.2	35.0	57.5	98.0	188.
		30	13.9	15.7	19.0	24.5	34.8	52.5	86.0	150.	285.
	35	0	4.42	5.15	6.38	8.39	11.7	17.2	27.1	45.8	84.1
		10	7.14	8.18	10.1	13.2	19.2	28.4	44.8	75.8	139.
		20	10.9	12.4	15.2	19.7	28.3	43.0	69.0	122.	225.
		30	16.0	18.1	22.0	28.5	40.0	22.6	102.	180.	350.
40	0	0	2.98	3.01	3.22	3.67	4.60	6.41	9.70	16.1	29.8
		10	3.51	3.66	4.13	5.04	6.68	9.58	14.9	25.5	48.3
		20	4.65	4.88	5.66	7.20	9.68	14.3	22.8	39.8	70.0
		30	6.11	6.59	7.70	10.0	14.0	21.0	34.2	60.5	110.
		40	7.97	8.30	9.80	12.8	19.2	30.3	52.0	91.0	162.
	5	0	3.12	3.22	3.54	4.21	5.56	7.97	12.4	21.1	39.9
		10	3.94	4.20	4.87	6.14	8.35	12.3	19.6	34.2	65.6
		20	5.38	5.84	6.94	9.0	12.4	18.7	30.5	53.9	102.
		30	7.35	8.12	9.60	12.5	18.2	28.1	46.4	82.9	150.
		40	9.89	10.5	12.6	16.5	25.0	41.1	68.0	132.	230.

Table 6 Passive Earth Pressure Coefficients $K_{p\gamma}$

φ	δ	β	α 50	60	70	80	90	100	110	120	130
40	10	0	3.30	3.49	3.96	4.96	6.76	9.94	15.8	27.6	52.8
		10	4.46	4.87	5.81	7.50	10.4	15.7	25.6	45.2	87.8
		20	6.29	7.01	8.53	11.2	15.9	24.4	40.3	72.0	135.
		30	8.87	10.0	12.0	16.2	23.6	37.0	61.8	111.	210.
		40	12.3	13.5	15.3	21.8	33.0	52.5	90.0	165.	315.
	15	0	3.53	3.84	4.55	5.91	8.25	12.4	20.2	35.6	69.0
		10	5.06	5.68	6.95	9.19	13.1	20.0	33.0	59.0	115.
		20	7.42	8.44	10.5	14.0	20.3	31.5	52.6	94.7	185.
		30	10.7	12.3	15.7	20.8	31.0	48.5	81.1	147.	280.
		40	15.2	17.0	21.0	29.0	47.0	70.0	120.	225.	430.
	20	0	3.82	4.30	5.31	7.06	10.1	15.4	25.5	45.5	88.9
		10	5.80	6.68	8.35	11.2	16.3	25.3	43.0	80.0	155.
		20	8.77	10.2	12.8	17.3	25.6	40.2	70.0	127.	250.
		30	12.9	15.2	19.5	26.4	41.0	63.0	106.	190.	350.
		40	18.7	21.4	27.0	37.9	60.0	94.5	164.	295.	550.
	25	0	4.21	4.92	6.23	8.45	12.3	19.1	31.8	57.3	113.
		10	6.70	7.87	10.0	13.7	20.1	31.6	56.0	102.	201.
		20	10.4	12.2	15.7	21.5	32.0	50.6	88.5	165.	300.
		30	15.6	18.5	23.8	33.0	49.0	78.0	132.	248.	450.
		40	22.8	27.0	35.0	49.0	74.0	120.	210.	375.	700.
	30	0	4.71	5.67	7.31	10.1	14.8	23.3	39.3	71.1	140.
		10	7.75	9.26	12.0	16.6	24.6	40.0	69.7	127.	251.
		20	12.2	14.6	19.0	26.5	39.5	64.0	114.	220.	400.
		30	18.7	22.5	29.0	44.0	62.0	100.	170.	315.	600.
		40	27.7	36.5	43.0	60.0	93.0	150.	260.	475.	920.
	35	0	5.33	6.52	8.54	11.9	17.8	28.2	47.7	86.6	171.
		10	8.95	10.8	14.2	19.9	30.0	50.0	88.0	160.	320.
		20	14.4	17.4	22.8	32.5	50.0	82.0	150.	290.	600.
		30	22.2	26.9	34.5	48.5	75.0	120.	210.	388.	760.
		40	32.0	38.5	51.0	72.0	108.	177.	310.	565.	1120
	40	0	6.01	7.45	9.88	13.9	20.9	33.3	56.6	103.	204.
		10	10.2	12.6	16.6	23.4	36.0	59.4	101.	190.	365.
		20	16.6	20.3	26.8	38.5	59.5	100.	184.	360.	780.
		30	26.0	31.7	40.5	56.8	91.0	150.	265.	485.	950.
		40	36.5	44.0	59.5	82.0	125.	215.	375.	700.	1330

Table 7 Active Earth Pressure Coefficients $K_{a\gamma}$

Angle of internal friction φ(deg)	Wall friction angle δ(deg)	Backfill angle β(deg)	Wall Angle α (deg.)								
			50	60	70	80	90	100	110	120	130
10	0	0	1.11	.943	.832	.756	.704	.669	.650	.641	.641
		10	1.41	1.20	1.06	.982	.937	.922	.900	.895	.890
	5	0	1.09	.917	.801	.720	.664	.626	.601	.586	.577
		10	1.45	1.23	1.08	1.00	.951	.936	.920	.900	.890
	10	0	1.07	.911	.787	.702	.642	.600	.570	.549	.533
		10	1.53	1.29	1.13	1.05	.991	.966	.950	.940	.935
15	0	0	1.02	.850	.735	.651	.589	.541	.504	.472	.438
		10	1.27	1.04	.893	.782	.701	.643	.595	.555	.516
	5	0	1.00	.828	.709	.622	.557	.507	.467	.433	.395
		10	1.28	1.04	.885	.764	.679	.612	.560	.516	.442
	10	0	1.00	.821	.695	.603	.536	.484	.442	.405	.365
		10	1.32	1.07	.889	.758	.663	.591	.536	.489	.473
	15	0	1.02	.826	.691	.596	.525	.470	.425	.385	.342
		10	1.38	1.11	.903	.760	.657	.581	.522	.471	.420
20	0	0	.937	.767	.647	.559	.490	.434	.387	.341	.290
		10	1.15	.920	.765	.653	.568	.500	.441	.387	.329
		20	1.44	1.17	1.01	.901	.822	.781	.759	.749	.732
	5	0	.921	.748	.626	.536	.465	.409	.361	.314	.263
		10	1.14	.915	.754	.634	.546	.474	.414	.360	.301
		20	1.47	1.19	1.03	.907	.840	.786	.763	.741	.736
	10	0	.924	.742	.614	.520	.448	.391	.342	.295	.243
		10	1.17	.926	.751	.626	.531	.457	.396	.340	.280
		20	1.51	1.23	1.06	.937	.855	.812	.776	.767	.748
	15	0	.942	.745	.610	.512	.438	.379	.328	.280	.229
		10	1.21	.949	.756	.622	.523	.446	.383	.325	.265
		20	1.59	1.29	1.11	.982	.895	.837	.813	.789	.769
	20	0	.970	.759	.614	.511	.434	.372	.319	.270	.217
		10	1.29	.984	.771	.626	.521	.441	.375	.315	.253
		20	1.72	1.39	1.18	1.04	.951	.888	.848	.821	.800
25	0	0	.859	.688	.568	.478	.406	.346	.293	.241	.184
		10	1.03	.814	.661	.549	.462	.389	.327	.267	.203
		20	1.25	1.00	.818	.681	.569	.480	.401	.326	.249
	5	0	.848	.674	.552	.459	.387	.327	.275	.223	.168
		10	1.03	.810	.648	.532	.443	.370	.308	.249	.186
		20	1.27	1.00	.824	.673	.557	.462	.381	.307	.230
	10	0	.851	.671	.542	.448	.374	.313	.261	.210	.156
		10	1.05	.814	.645	.523	.431	.356	.294	.235	.173
		20	1.31	1.03	.830	.673	.548	.449	.367	.292	.216

Table 7 Active Earth Pressure Coefficients $K_{a\gamma}$

			α								
φ	δ	β	50	60	70	80	90	100	110	120	130
25	15	0	.866	.672	.540	.441	.365	.304	.251	.200	.146
		10	1.09	.828	.647	.520	.423	.347	.284	.225	.164
		20	1.37	.107	.853	.678	.545	.441	.357	.282	.206
	20	0	.896	.685	.542	.439	.361	.298	.244	.193	.139
		10	1.14	.856	.658	.521	.420	.342	.277	.217	.156
		20	1.45	1.12	.886	.688	.545	.438	.351	.274	.198
	25	0	.925	.725	.552	.443	.361	.296	.240	.187	.134
		10	1.22	.920	.676	.528	.423	.341	.273	.212	.151
		20	1.56	1.20	.929	.708	.554	.439	.349	.270	.192
30	0	0	.787	.617	.497	.406	.333	.272	.218	.165	.108
		10	.929	.717	.569	.460	.373	.301	.239	.180	.116
		20	1.12	.861	.683	.546	.438	.353	.276	.207	.135
		30	1.38	.107	.899	.765	.684	.610	.561	.500	.434
	5	0	.778	.606	.484	.392	.319	.258	.205	.154	.099
		10	.932	.715	.559	.446	.359	.287	.226	.168	.108
		20	1.12	.861	.678	.536	.426	.338	.263	.194	.125
		30	1.39	1.09	.912	.776	.694	.619	.570	.507	.428
	10	0	.781	.604	.477	.383	.309	.248	.196	.145	.093
		10	.946	.720	.557	.439	.349	.277	.216	.159	.100
		20	1.16	881.	.681	.532	.419	.328	.252	.184	.117
		30	1.43	1.14	.934	.795	.712	.634	.570	.506	.426
	15	0	.798	.607	.475	.378	.302	.242	.189	.138	.087
		10	.972	.728	.558	.437	.343	.270	.209	.152	.095
		20	1.19	.900	.695	.532	.414	.321	.245	.177	.111
		30	1.51	1.18	.968	.823	.738	.657	.590	.524	.442
	20	0	.821	.618	.479	.377	.299	.237	.184	.134	.083
		10	1.01	.750	.566	.437	.341	.266	.204	.147	.091
		20	1.25	.943	.712	.539	.414	.318	.240	.172	.106
		30	1.59	1.24	1.01	.885	.773	.688	.618	.549	.448
	25	0	.862	.638	.487	.380	.299	.235	.180	.130	.080
		10	1.08	.785	.581	.442	.342	.265	.201	.143	.087
		20	1.35	1.00	.739	.550	.418	.318	.238	.169	.103
		30	1.74	1.35	1.11	.940	.820	.729	.654	.564	.473
	30	0	.900	.770	.501	.387	.302	.236	.179	1.27	.078
		10	1.17	.829	.602	.453	.347	.266	.200	.141	.085
		20	1.47	1.08	.776	.568	.425	.321	.238	.167	.100
		30	1.88	1.46	1.19	1.01	.882	.783	.701	.604	.489
35	0	0	.717	.551	.433	.343	.271	.211	.158	.107	.057
		10	.837	.634	.491	.383	.299	.230	.171	.115	.060
		20	.986	.741	.572	.443	.342	.261	.191	.128	.066

Table 7 Active Earth Pressure Coefficients $K_{a\gamma}$

φ	δ	β	α 50	60	70	80	90	100	110	120	130
35	0	30	1.18	.895	.703	.558	.434	.331	.240	.160	.084
	5	0	.711	.542	.424	.333	.260	.201	.149	.101	.052
		10	.843	.629	.483	.372	.289	.220	.162	.108	.056
		20	1.01	.741	.568	.435	.333	.250	.182	.120	.060
		30	1.20	.904	.708	.557	.426	.320	.230	.151	.078
	10	0	.717	.543	.418	.326	.253	.194	.143	.095	.049
		10	.849	.635	.480	.368	.282	.213	.155	.103	.052
		20	1.02	.759	.569	.430	.326	.243	.175	.115	.057
		30	1.22	.923	.720	.560	.422	.312	.222	.145	.074
	15	0	.731	.546	.417	.322	.248	.189	.138	.091	.046
		10	.876	.643	.481	.365	.277	.208	.150	.098	.049
		20	1.05	.775	.575	.430	.322	.238	.170	.110	.054
		30	1.27	.975	.753	.567	.421	.308	.216	.140	.070
	20	0	.755	.557	.420	.322	.246	.186	.135	.088	.044
		10	.915	.664	.488	.367	.275	.205	.147	.095	.047
		20	1.11	.800	.592	.434	.322	.235	.166	.107	.052
		30	1.36	1.02	.781	.580	.424	.306	.214	.137	.068
	25	0	.791	.575	.430	.325	.246	.185	.133	.086	.043
		10	.968	.692	.501	.371	.276	.204	.145	.093	.046
		20	1.17	.847	.610	.443	.323	.235	.165	.105	.050
		30	1.44	1.08	.819	.598	.429	.307	.213	.134	.066
	30	0	.846	.601	.442	.331	.249	.185	.132	.085	.042
		10	1.04	.730	.519	.379	.280	.205	.144	.092	.044
		20	1.27	.908	.637	.455	.329	.237	.164	.103	.049
		30	1.60	1.15	.870	.623	.438	.310	.213	.133	.064
	35	0	.928	.634	.460	.341	.254	.187	.132	.084	.041
		10	1.12	.783	.545	.392	.287	.208	.145	.091	.044
		20	1.41	.989	.676	.473	.337	.241	.166	.103	.048
		30	1.75	1.29	.951	.656	.457	.318	.216	.134	.064
40	0	0	.649	.491	.374	.287	.217	.160	.111	.065	.024
		10	.760	.556	.421	.316	.237	.172	.118	.069	.025
		20	.874	.643	.482	.358	.266	.191	.129	.075	.026
		30	1.38	.762	.577	.429	.316	.226	.150	.086	.029
		40	1.22	.920	.751	.614	.511	.443	.364	.277	.160
	5	0	.645	.486	.368	.279	.210	.153	.105	.061	.022
		10	.759	.553	.415	.310	.230	.166	.112	.064	.023
		20	.879	.644	.479	.352	.259	.183	.123	.070	.024
		30	1.03	.770	.579	.426	.309	.218	.143	.081	.027
		40	1.25	.941	.769	.628	.524	.439	.361	.274	.157

Table 7 Active Earth Pressure Coefficients $K_{a\gamma}$

φ	δ	β	α 50	60	70	80	90	100	110	120	130
40	10	0	.654	.485	.364	.275	.205	.149	.101	.058	.021
		10	.767	.562	.413	.305	.225	.160	.108	.061	.022
		20	.894	.651	.480	.349	.254	.178	.118	.067	.023
		30	1.05	.786	.586	.425	.305	.212	.139	.078	.026
		40	1.29	.973	.769	.650	.542	.455	.374	.273	.155
	15	0	.664	.490	.365	.272	.201	.145	.098	.056	.020
		10	.783	.571	.415	.304	.221	.157	.105	.059	.021
		20	.937	.666	.486	.349	.251	.175	.115	.065	.022
		30	1.07	.811	.590	.426	.304	.209	.135	.075	.024
		40	1.35	1.02	.804	.657	.567	.459	.377	.286	.154
	20	0	.690	.503	.367	.273	.200	.143	.096	.054	.019
		10	.822	.585	.421	.306	.220	.155	.103	.057	.020
		20	.975	.688	.496	.352	.250	.173	.113	.063	.021
		30	1.11	.846	.610	.434	.305	.208	.133	.073	.023
		40	1.43	1.08	.849	.693	.578	.485	.399	.290	.155
	25	0	.717	.518	.376	.276	.200	.143	.095	.053	.018
		10	.860	.607	.431	.310	.221	.155	.101	.056	.019
		20	1.03	.729	.511	.359	.252	.173	.112	.061	.020
		30	1.17	.892	.637	.445	.309	.208	.132	.072	.023
		40	1.53	1.15	.908	.741	.617	.518	.409	.297	.156
	30	0	.765	.543	.388	.281	.203	.143	.094	.052	.018
		10	.927	.643	.447	.317	.224	.156	.101	.055	.019
		20	1.10	.772	.532	.369	.256	.174	.112	.061	.020
		30	1.24	.953	.681	.463	.314	.210	.133	.071	.022
		40	1.67	1.25	.984	.802	.668	.559	.442	.321	.160
	35	0	.840	.576	.405	.289	.207	.145	.094	.052	.017
		10	1.02	.690	.470	.327	.230	.158	.102	.055	.018
		20	1.22	.840	.562	.383	.263	.177	.113	.060	.020
		30	1.33	1.03	.727	.480	.324	.214	.134	.071	.023
		40	1.84	1.38	1.08	.881	.733	.589	.463	.335	.164
	40	0	.946	.598	.428	.302	.214	.148	.096	.052	.017
		10	1.09	.738	.500	.342	.238	.162	.103	.055	.018
		20	1.38	.931	.604	.402	.273	.182	.114	.061	.019
		30	1.50	1.17	.792	.512	.338	.221	.136	.072	.023
		40	2.07	1.55	1.21	.985	.817	.654	.513	.353	.171

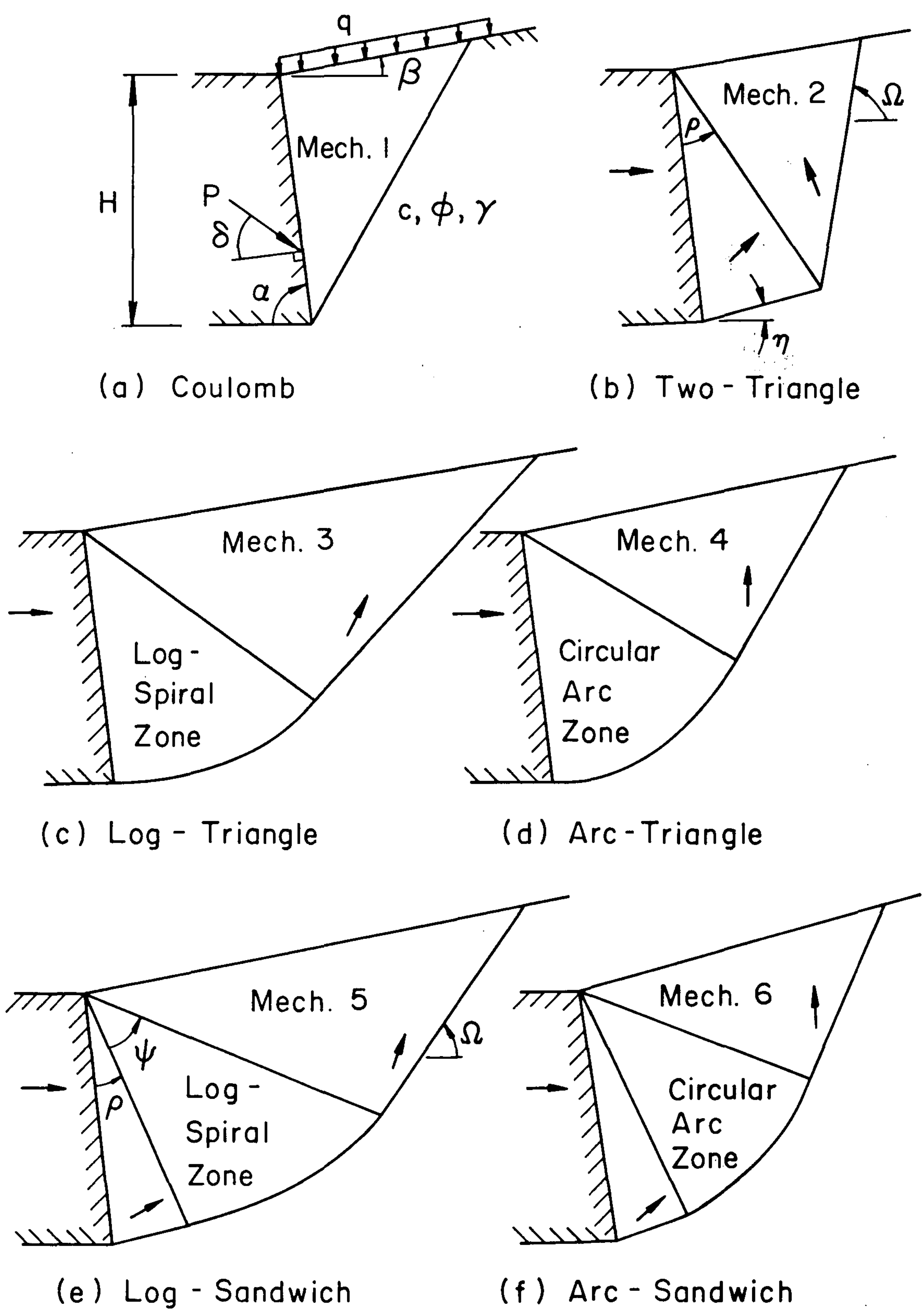

Fig. 1 Failure Mechanisms

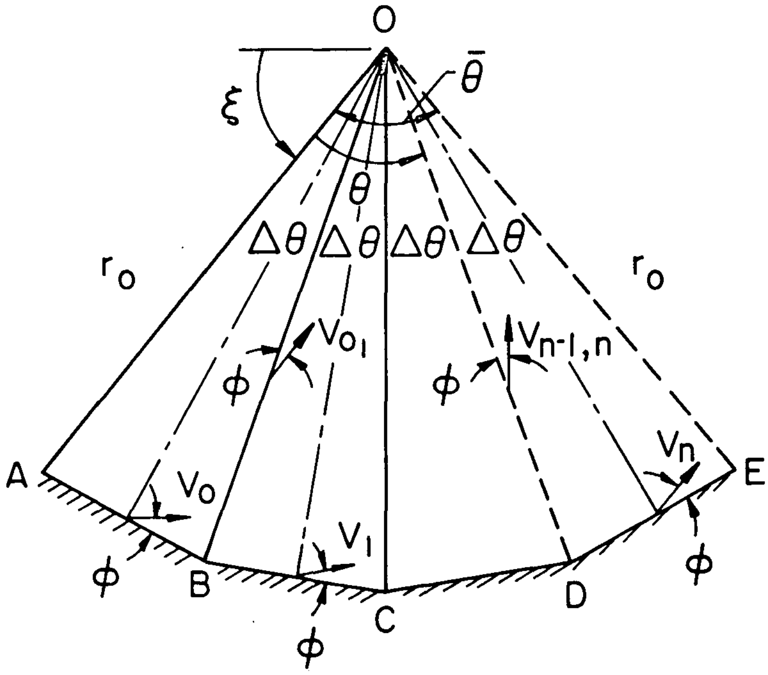

(a) Division of Zone Into n Rigid Triangles

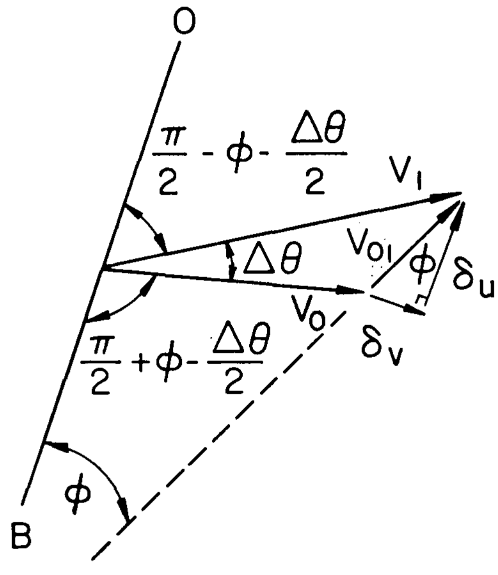

(b) Velocity Diagram for Regions AOB and BOC

Fig. 2 Circular Shearing Zone ($\varphi \neq 0$)

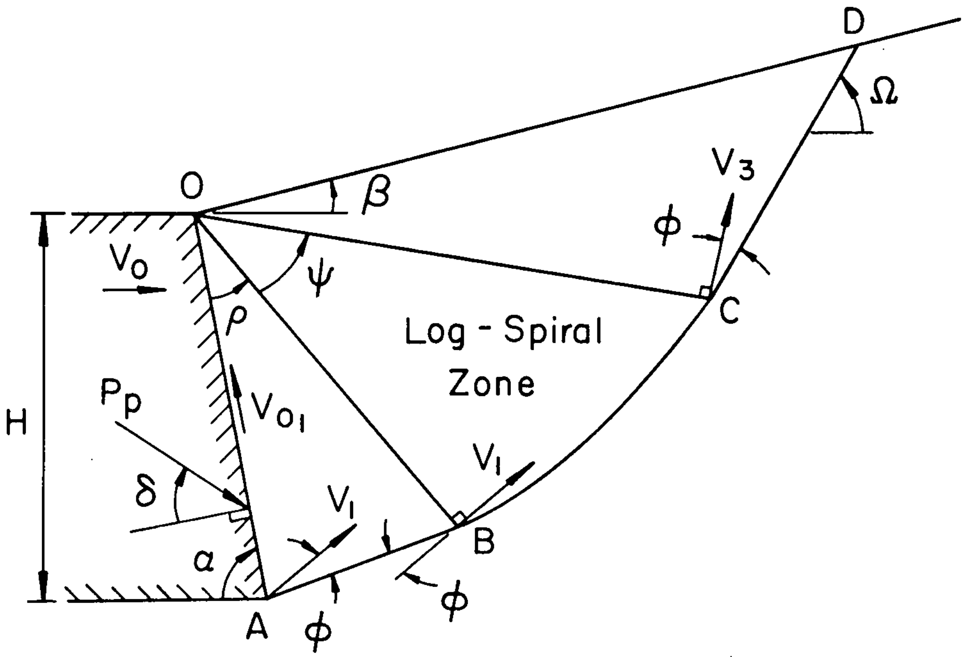

(a) $V_3 = V_1 \exp(\psi \tan\phi)$

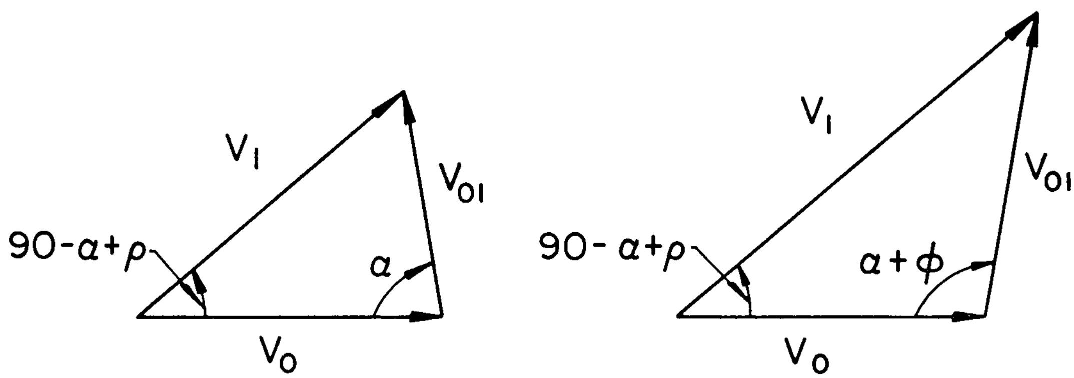

(b) Smooth Wall $\delta < \phi$ (c) Rough Wall $\delta = \phi$

Fig. 3 Passive Log-Sandwich Mechanism

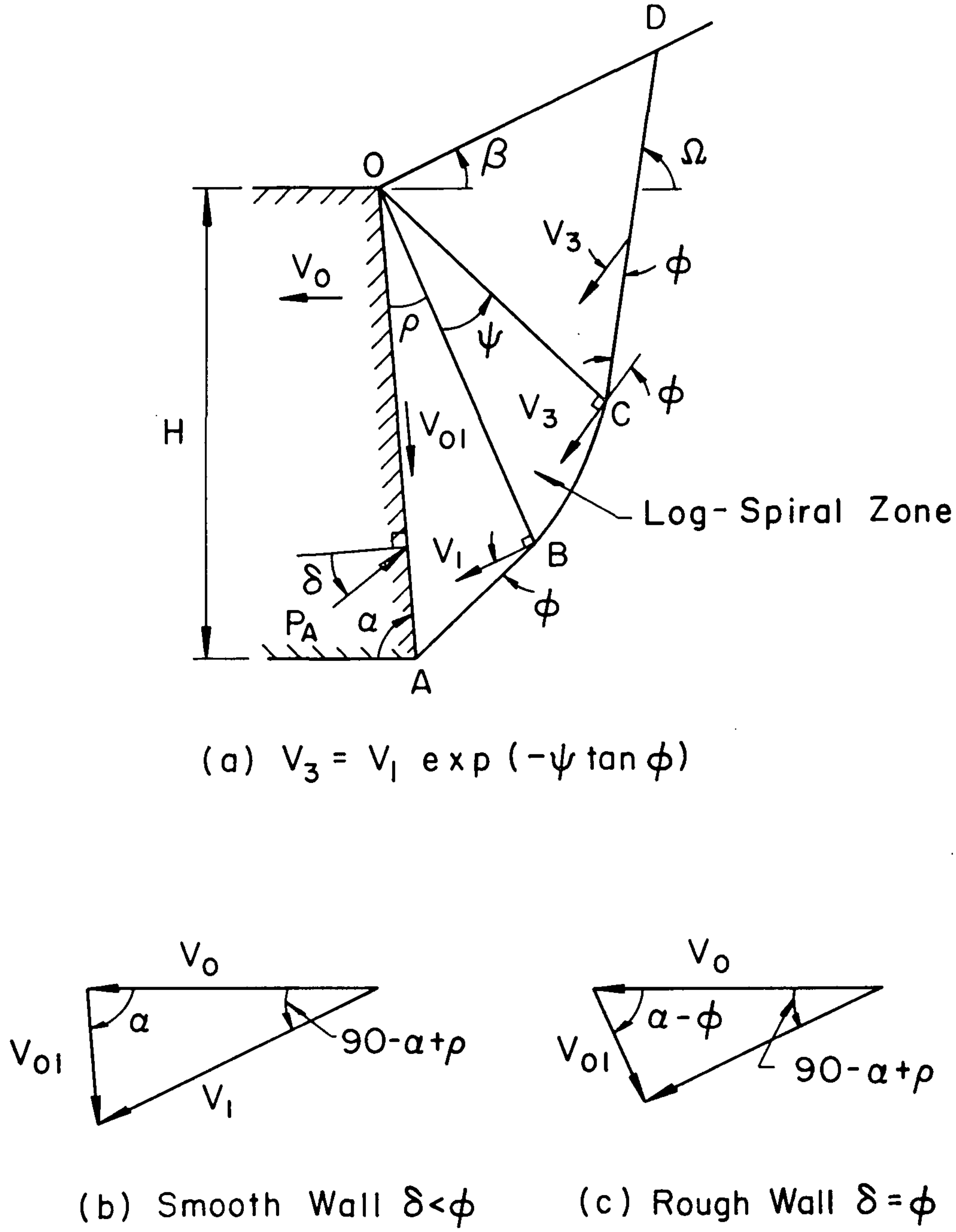

Fig. 4 Active Log-Sandwich Mechanism

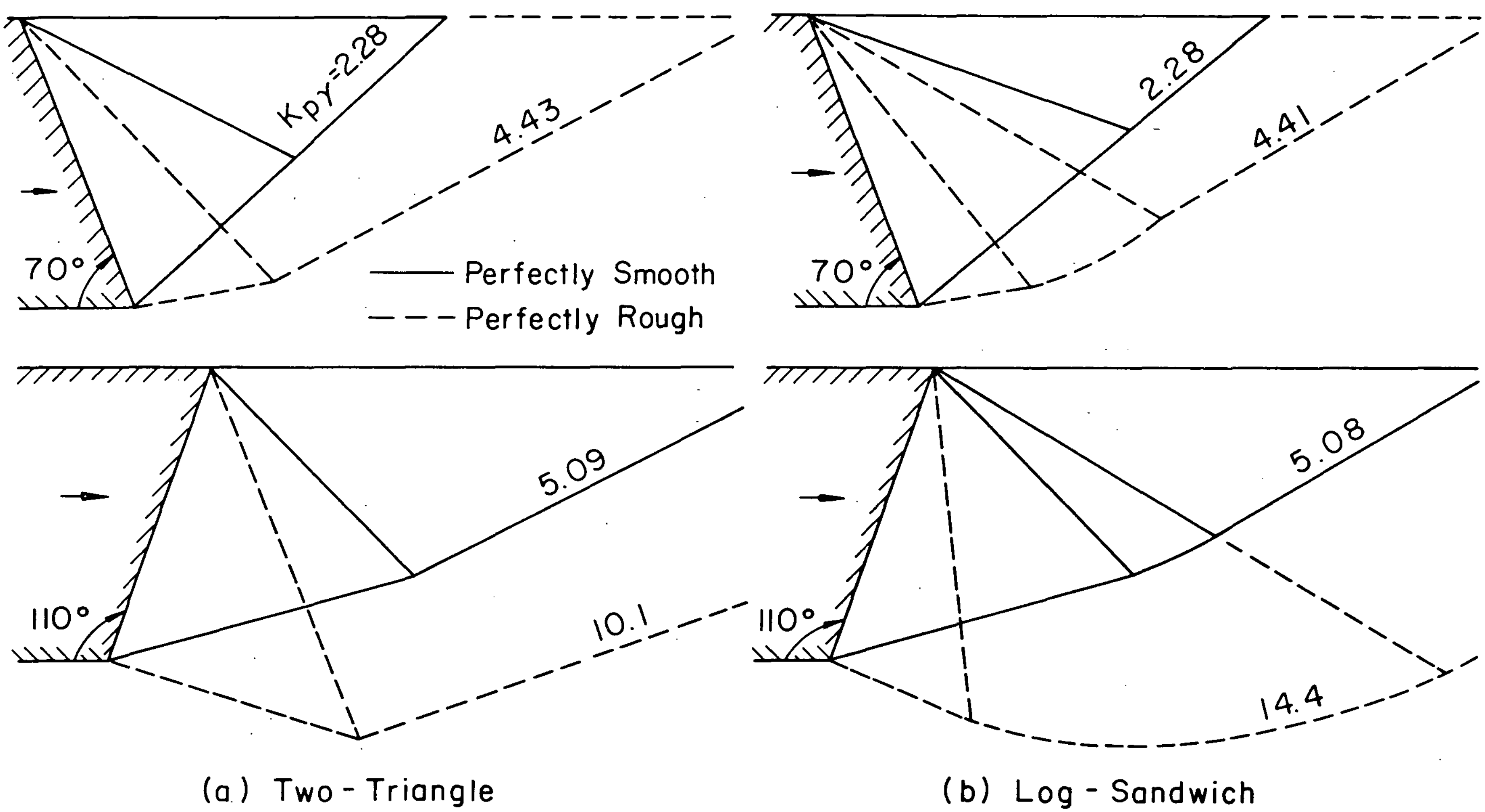

Fig. 5 Typical Passive Mechanism Results (φ = 30°)

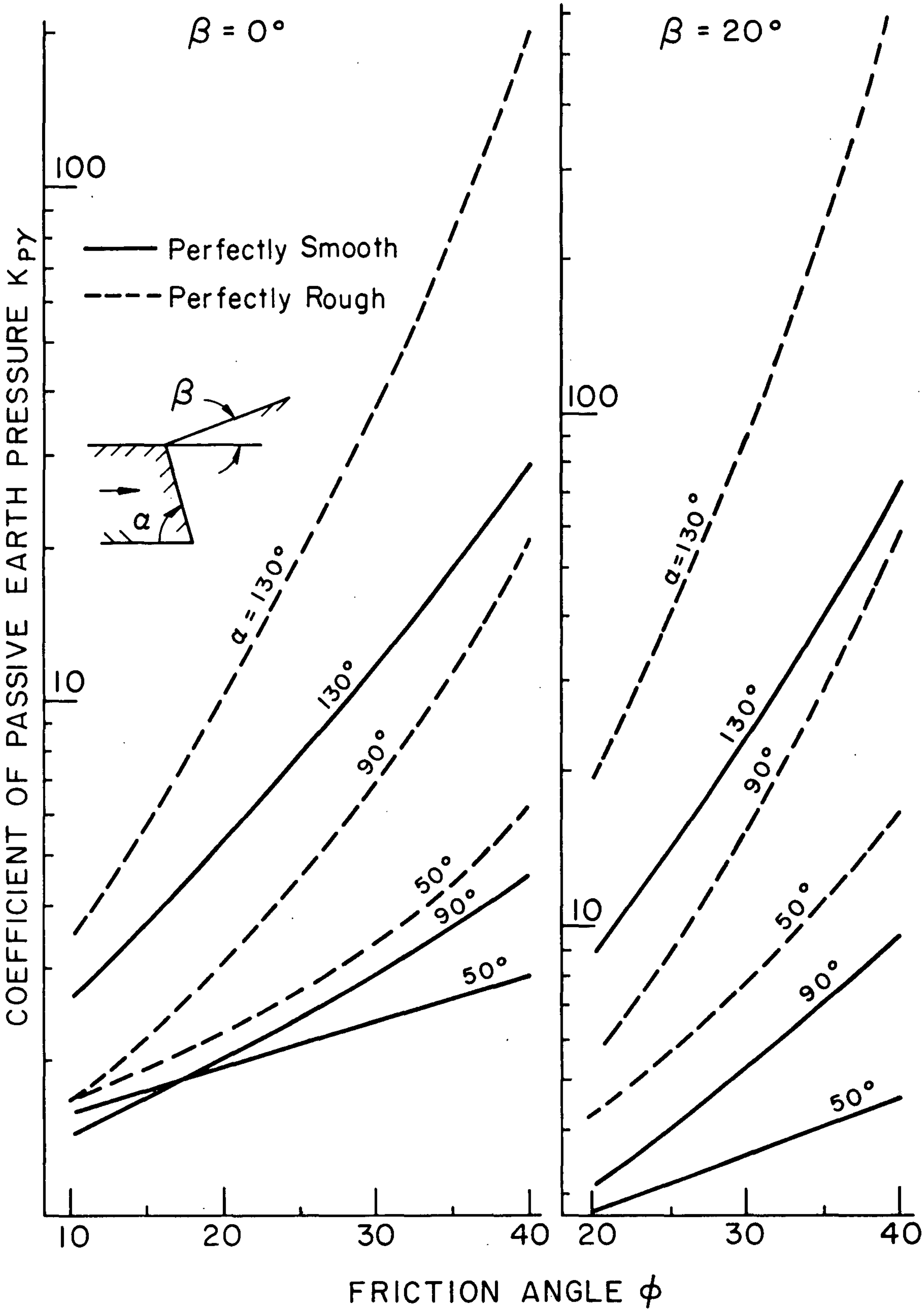

Fig. 6 Effect of Wall Roughness on Passive Pressure

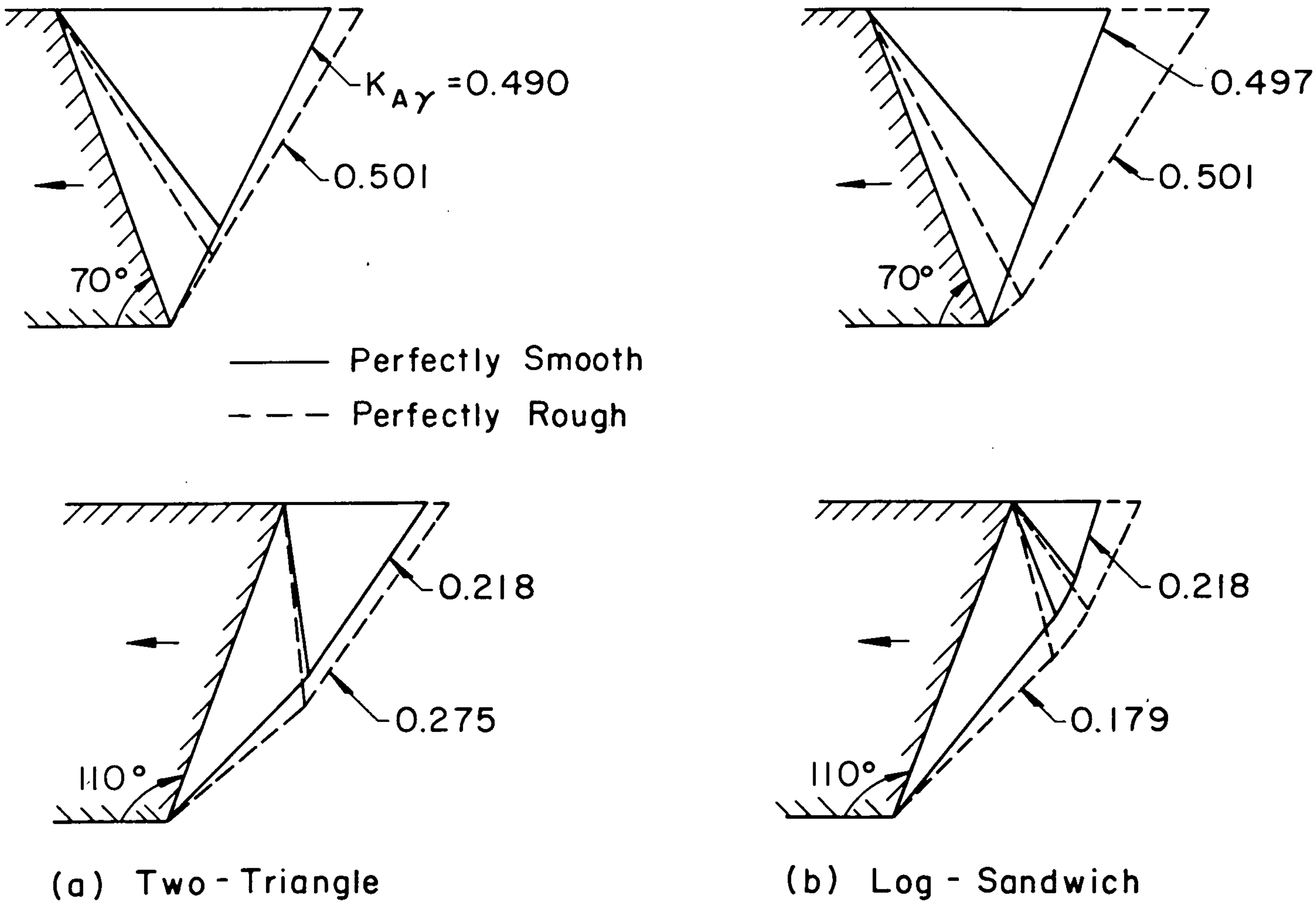

Fig. 7 Typical Active Mechanism Results ($\varphi = 30^{\circ}$)

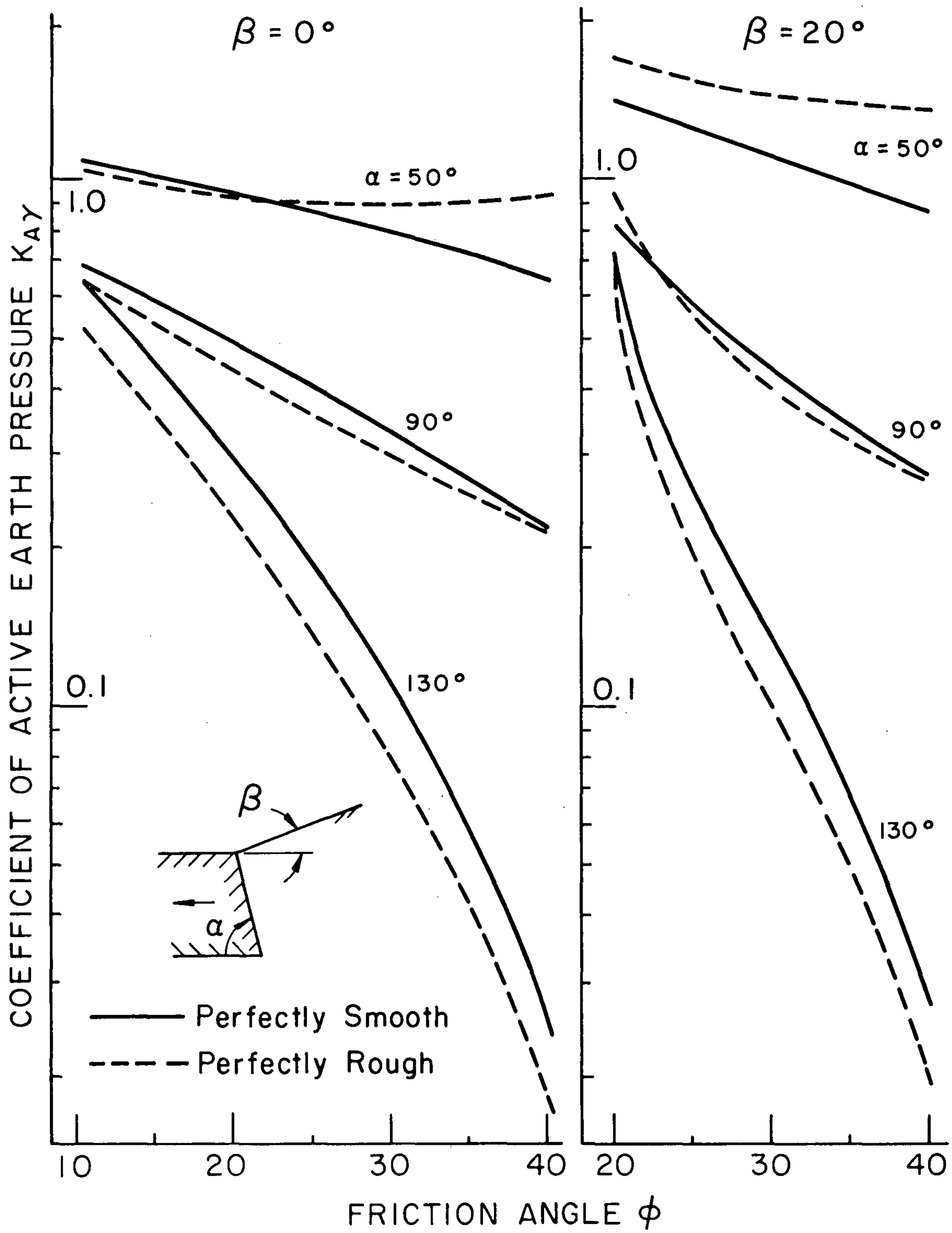

Fig. 8 Effect of Wall Roughness on Active Pressure

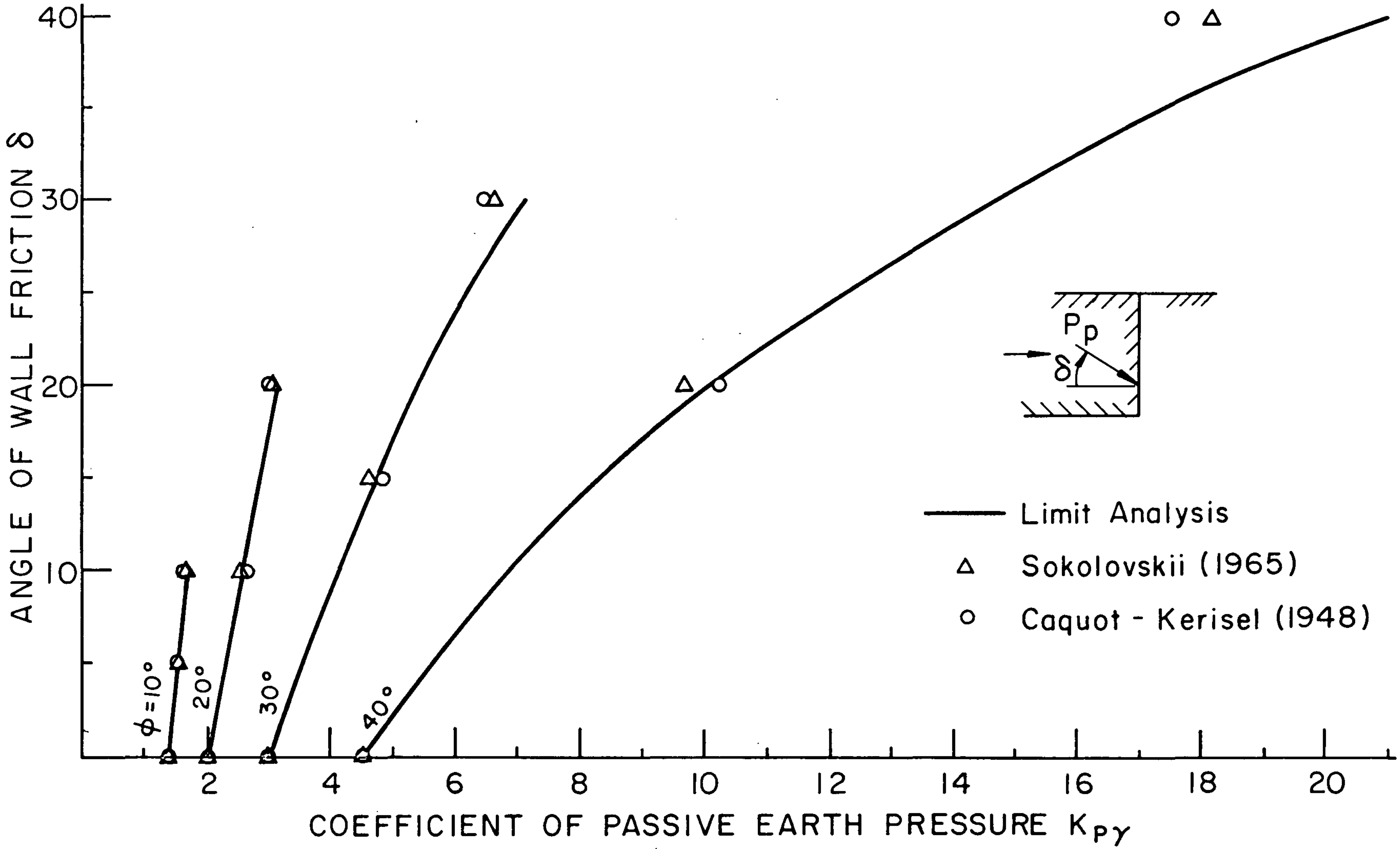

Fig. 9 Passive Earth Pressure $\alpha = 90^{\circ}$ $\beta = 0^{\circ}$

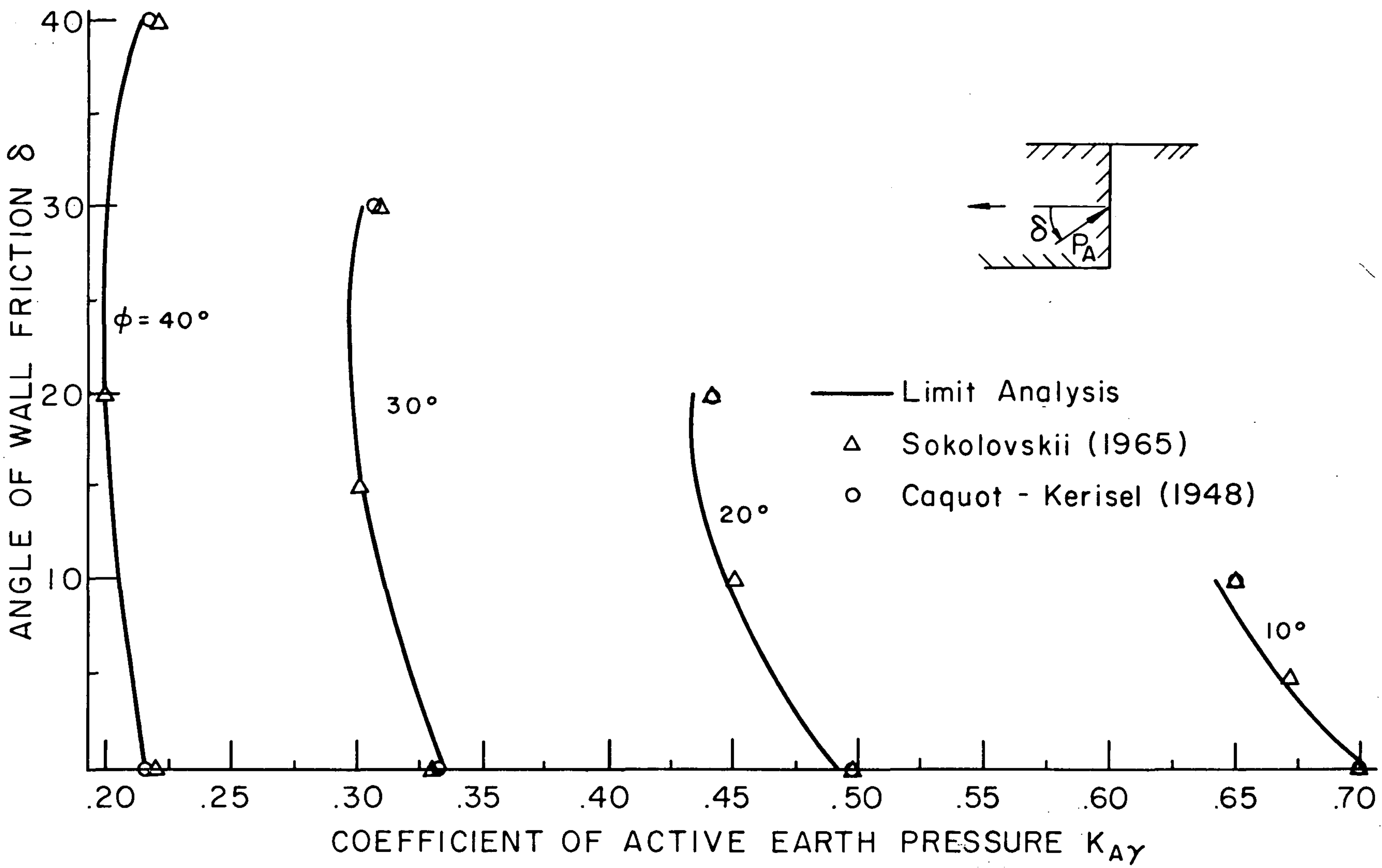

Fig. 10 Active Earth Pressure $\alpha = 90^o$ $\beta = 0^o$

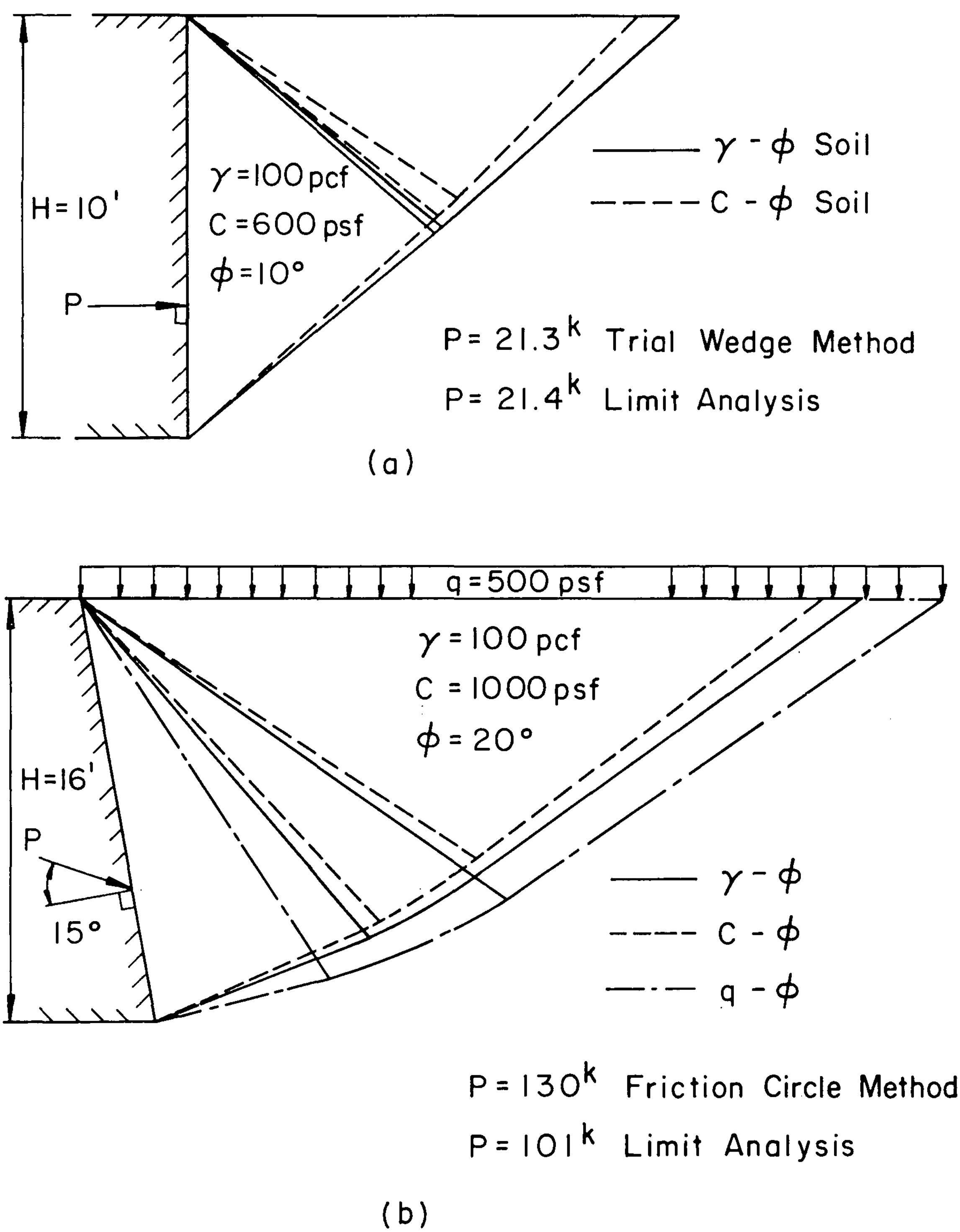

Fig. 11 Inclusion of Cohesion and Surcharge Loading

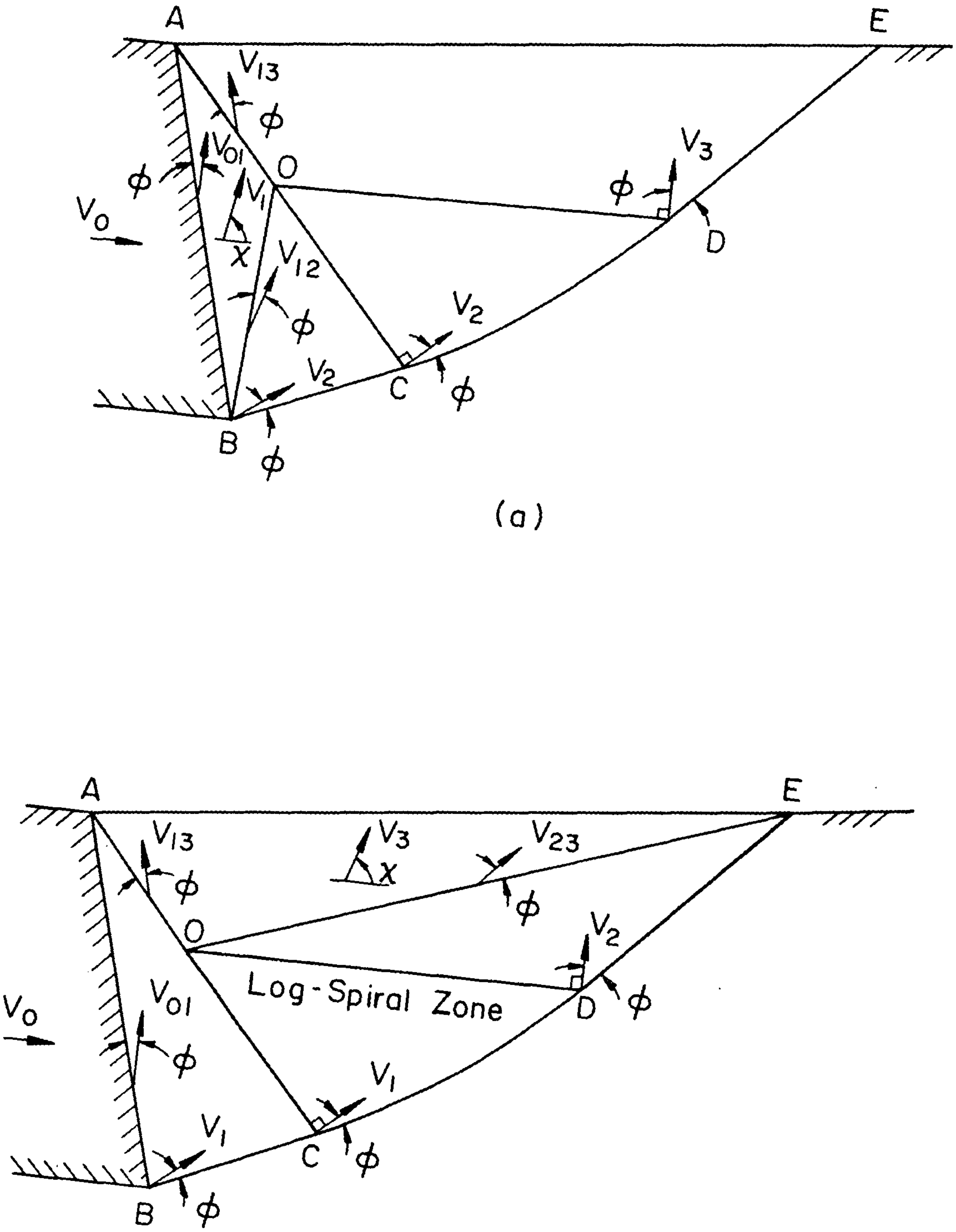

Fig. 12 General Passive Log-Sandwich Mechanism with Shifting Pole

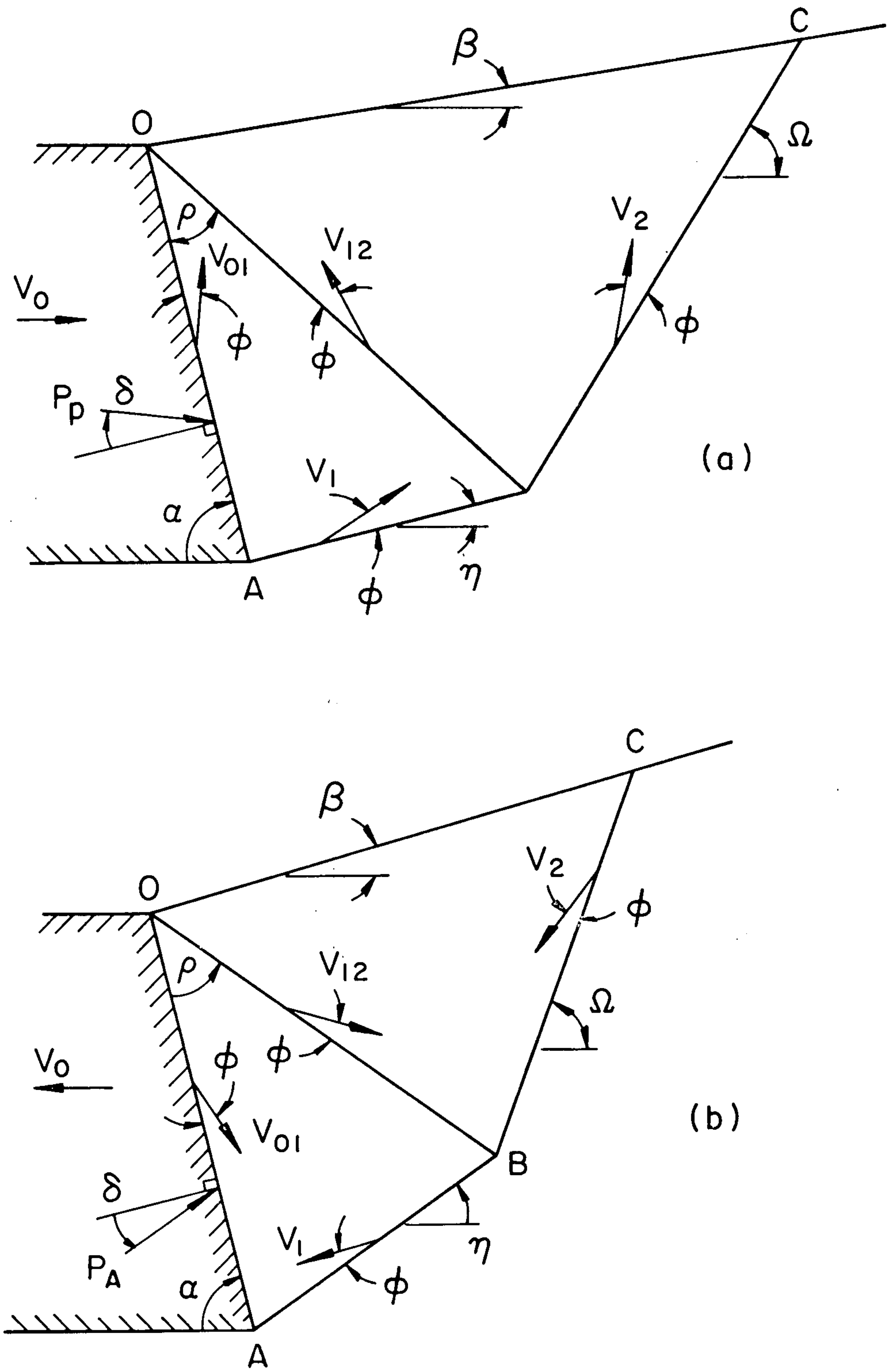

Fig. 13 Two-Triangle Mechanism